ashoka UNIVERSITY
CENTRE FOR A
People-centric
Energy Transition

Strategies to Address India's Critical Minerals' Vulnerability through Resource Efficiency

Contributors:

Animesh Ghosh, Research Fellow, ACPET
Soumit Pandey, Junior Research Associate, ACPET
Vaibhav Chowdhary, Director, ACPET
Anvesha Adhikari, Junior Research Associate, ACPET

Abstract

India's clean energy transition is essential for achieving its ambitious climate targets, including 500 GW of non-fossil fuel capacity by 2030 and net-zero emissions by 2070. This transition necessitates a significant supply of critical minerals (CMs) essential for manufacturing renewable energy (RE) technologies such as solar, wind, battery storage systems, and green hydrogen electrolysers. This study projects the demand for 31 CMs across five RE segments - Solar Photovoltaics (PV), Concentrating Solar Power (CSP), Wind (onshore & offshore), stationary Battery Energy Storage Systems (BESS) and Green Hydrogen Electrolysers - until 2070.

Using new (Year-on-Year) capacity values for the Business-as-usual and Heroic (Net-Zero) scenarios from India Energy Security Scenarios (IESS) 4.0, the study employs a technological assessment framework, material intensity analysis, and market share projections to estimate mineral requirements. Findings indicate that Copper, Nickel, Silicon, Graphite, Vanadium, Phosphorous, Rare-Earth Elements (REEs), and Lithium will see substantial growth in demand.

The study highlights the aggressive growth of year-on-year as well as cumulative demand/requirement of each CM until 2070 across the above-listed RE segments to portray the need for a comprehensive strategy, including resource efficiency, domestic mineral exploration, recycling initiatives, and international collaborations, to mitigate supply vulnerabilities and support India's sustainable energy future.

Keywords: PV, CSP, Wind, BESS, Electrolyser, Capacity, Mineral, Demand

Highlights

- Technological Assessment Framework
- Heuristic Approach to determine Market Share of clean energy technologies
- Demand Assessment Framework till 2070, India’s Net-Zero target year.
- Introduction and demand assessment modelling of Perovskite solar PV technologies
- Introduction and demand assessment modelling of 7 sodium-ion stationary BESS technologies
- Demand assessment modelling of Electrolysers required for Green Hydrogen production
- Significant reduction of Cobalt’s (a geopolitically sensitive and toxic mineral) demand

Contents

1. Introduction: Background, Problem Statement, Literature Review

India's clean energy transition is critical for achieving its climate goals of 500 GW [1] of non-fossil fuel capacity by 2030 and net-zero emissions by 2070 [2]. This transition demands substantial quantities of critical minerals (CM) [3] which are essential for manufacturing RE systems like solar, wind, energy storage systems, and green hydrogen electrolysers. The Ministry of Mines, Government of India, has identified 30 CMs [4] essential for national security and economic growth. Given their scarcity, addressing the growing demand for these minerals has become crucial in India's transition to a low-emission economy and in achieving its 'Net Zero' targets to successfully meet its renewable energy ambitions and foster a sustainable development future.

In this study, project the demand for the CMs required in various Solar Photovoltaics (PV), Concentrating Solar Power (CSP), Wind (onshore & offshore), stationary Battery Energy Storage Systems (BESS) and Green Hydrogen Electrolysers technologies, from 2025 to 2070, based on the year-on-year (YoY) installed capacity of RE plants given in the Business-as-usual (BAU) Scenario and Heroic or Net-Zero (NZ) Scenario of India Energy Security Scenarios (IESS). In the computation exercise conducted by ACPET, 23 CMs from the 30 listed by the Ministry of Mines have been analyzed across all RE segments. Among these 30 CMs, two categories, REEs and Platinum Group Elements (PGEs), encompass multiple individual minerals. Specifically, the Ministry of Mines lists 17 minerals under REEs and 6 under PGEs, bringing the total number of critical minerals to 51. This study covers 31 of these 51 CMs, including Cadmium, Cobalt, Copper, Gallium, Germanium, Graphite, Indium, Lithium, Molybdenum, Niobium, Nickel, Phosphorous, Selenium, Silicon, Strontium, Tellurium, Tin, Titanium, Tungsten, Vanadium and Zirconium. Among the REEs, Dysprosium, Neodymium, Praseodymium, Terbium, Yttrium, Cerium, Lanthanum, and Gadolinium have been included, while among the PGEs, Platinum and Iridium have been covered. This comprehensive coverage ensures that the study captures the most relevant minerals essential for clean energy technologies and infrastructure.

This paper is structured into six segments – introduction, methodology, results and analysis, discussion, conclusion and appendix. The methodology deals with the process of the assessment of demand, while the results and analysis of the assessment. We conclude the paper with discussion and conclusion, where we attempt to understand the implications of the demand assessment results and try to develop a framework for future research. The data used for the assessment is given in the appendix section at the end.

2. Material & Methods

2.1. Technological Assessment Framework

In this study, 8 clean energy technologies (CETs) in Solar PV, 2 CETs in Solar CSP, 5 CETs in onshore Wind, 4 CETs in offshore Wind, 17 CETs in BESS, and 3 electrolysers for Green Hydrogen production, were selected to be part of the exercise, based on the Technology Readiness Level (TRL), Efficiency of technology, and End of Life (EOL) of technology, determined from systemic literature review. TRL indicates the maturity of the CETs. CETs with TRL level 4 to 9 have been selected for the exercise [5].

TRL = f (Validation Stage, Testing Environment, Integration Level, Documentation, Demonstration)

As for EOL of CETs, the CET that retire at least 20 years from the date of their commercialization has been considered.

Overall, 39 CETs have been considered for this demand/requirement projection exercise for CMs.

2.2. Assessment of the requirement of critical minerals in RE technologies for all the RE segments

This exercise considered RE segment-specific YoY capacities provided in India Energy Security Scenarios 2070, i.e., IESS Version 4.0. IESS Version 4.0 uses sector-specific levers categorised into four levels: Level 1 (Pessimistic), which assumes minimal interventions; Level 2 (Business-As-Usual or BAU), reflecting outcomes achievable based on historical and current trends; Level 3 (Optimistic/Deterministic), which aligns with national and international climate commitments; and Level 4 (Heroic/Net-Zero or NZ), targeting highly ambitious goals within technical feasibility. In this exercise, the demand for CMs was projected through a multi-step approach. To begin with, the annual requirement of each CM was estimated for every CET under all RE segments, under both BAU and NZ scenarios, over the period 2025–2070. This was based on YoY capacity additions from IESS of each RE segment, the market share of each CET under each RE segment, and the mineral intensity of each CM in each CET. Subsequently, the annual CM requirements were summed across all CETs within each RE segment to determine the total demand of each CM per RE segment per year. Further, these values were added across all RE segments to obtain the total annual demand for each CM. Finally, the total annual demand values were aggregated across the entire period to calculate the cumulative demand for every CM from 2030 to 2070. Refer to section 2.4 for the above calculations. We have used data from various studies on mineral intensity. Mineral intensity is measured in tonnes per gigawatt (t/GW) for renewable energy segments like Solar PV, CSP, and Wind. For BESS, it is measured in tonnes per gigawatt-hour (t/GWh). For data on Electrolysers, data on Green Hydrogen production projection in million tonnes (Mt) until 2070 has been provided by NITI Aayog, which has been considered along with the data on efficiency of the three electrolysers secured from literature, to generate YoY capacity values of the electrolysers in t/GW.

Data on the market share of CETs has been considered from various literature. However, many of these technologies are not fully commercialized yet. Due to this, the market share of these technologies is uncertain. Moreover, projection of the market share until 2070 was also not available in the literature. To address this data gap, we used a heuristic approach, where market share has been projected as a function of TRL, efficiency, and EOL of the CETs. TRL being a key factor, we have considered the assumption while projecting the market share that for CETs under any RE segment with TRL 8-9, the market share is to decrease over the years for all the trajectories gradually. On the other hand, for CETs with TRL level 4-7, the market share is to increase over the years, for all the trajectories gradually. This assumption comes from the idea that gradually, with time, the technologies will mature, causing their market share to increase. Due to this, the market share of CETs, which are mature at the current time, will fall gradually with time. This is because market share is given on a scale of 0 to 1, so with the increase in CETs under a RE segment in the market, the market share of each CET falls. It is to be noted that the market share of CETs also varies across trajectories. Table 3 in the annexure gives the market share of all the CETs under all the RE segments considered in this exercise.

3. Calculation

3.1. Year-on-Year Capacity

A ±10% variation has been applied to the YoY capacity values to account for the inherent uncertainty in projection-based exercises. Accordingly, Tables 2.1 and 2.2 in the annexure present a range of values for both the BAU and NZ scenarios, reflecting this ±10% margin. However, for the plotting exercise in Section 4 (Result and Analysis), the upper bound of this range has been used as the basis for visualization.

The updated version of IESS 4.0 provides YoY capacity values for Solar as a combined category, without separating Solar PV and CSP, unlike the earlier version which reported them individually. To estimate the separate YoY capacity values for Solar PV and CSP in the updated version, the values from the older version were first summed to calculate the total solar capacity. The share of Solar PV and CSP was then determined based on their respective proportions in this total. These proportions were subsequently applied to the combined solar capacity figures in the updated version to derive the separate new capacity values for Solar PV and CSP. The resulting disaggregated values are presented in Tables 2.1 and 2.2, while the applied proportions are shown in Table 2.3 of the annexure.

Equation 1 below gives the formula for generating capacity values [6] for electrolysers based on efficiency and green hydrogen production projection per annum.

$$\boldsymbol{X_{t_k}} = \frac{\boldsymbol{P_{t_k} * e_y * 10^9}}{\boldsymbol{8670 * 10^6}} \quad \textbf{……… (1)}$$

Where,

- X_{T,t_k} represents the capacity of Electrolyser in time period "k", where, $k \in \{2025-30, 2030-25, \ldots .2065-70\}$
- P_{T,t_k} is estimated Green Hydrogen Production in time period "k".
- e_y is the efficiency of electrolyser "y".
  Here, $y \in \{AEL, PEMEL, SOEL\}$.

We have followed the method in calculating the YoY capacity as given in Khan et al. (2024). The literature provided the Efficiency of Electrolyser "y" in $\frac{\text{KWh}}{\text{Kg}}$ and green hydrogen production in million tonnes for year "k". To convert this value to Kg, a factor of 10^9 is multiplied, and to convert KWh to GWh, the equation is divided by a factor of 10^6. To convert from GWh to GW, we divide by 8760 hours, that is, the total hours in a year.

Efficiency of AEL is 50 KWh/kg [6] of green hydrogen produced. Whereas efficiency of PEMEL is 60 KWh/Kg [6], and efficiency of SOEL is 37 KWh/Kg [7] of green hydrogen produced. Here, electrolyzer efficiencies represent the amount of electricity required to produce one unit of hydrogen, typically measured in kilowatt-hours (kWh) per kilogram (kg) of H_2

output. This metric indicates how efficiently an electrolyzer converts electrical energy into hydrogen, with lower values signifying higher efficiency.

3.2. Calculation of the year- on- year demand of critical minerals

We have assumed that mineral intensity remains constant over the years and across all trajectories, since that reductions in mineral intensity for selected technologies typically result from innovations driven by high mineral prices. However, since future prices are uncertain and influenced by various global supply and demand factors, it is challenging to estimate changes in mineral intensity at this stage.

Let "m" be the set of CMs, that is 31. Let "i" be the set of CETs across all the RE segment, that is, 39. Let "R" be the set of RE segments, that is 5. Finally, let "t" be the set of years, that is, 9. Thus, equation 2 given below describes the calculation for the YoY demand of a CM "j" in a CET "l" classified a RE segment "p" in year "k":

$$\boldsymbol{L_{m_j,i_l,R_p,t_k}} = \mu_{i_l,R_p,t_k} * \boldsymbol{N_{R_p,t_k}} * \boldsymbol{M_{m_j,i_l,R_p}} \text{ .... } \mathbf{(2)}$$

Where,

- $m = \{m_1 \text{..........}, m_n\}$; Where, $j = 1, \dots \dots, n$
- $i = \{i_1 \dots \dots, i_a\}$; Where, $l = 1, \dots \dots, a$
- $R = \{R_1 \dots \dots, R_b\}$; Where, $p = 1, \dots \dots, b$
- $t = \{t_1 \dots \dots, t_c\}$; Where, $k = 1, \dots \dots, c$
  $\Rightarrow t = \{t_1 \dots \dots, t_4\}$; Where, $k = 1, \dots \dots, 4$.
- "j" represents one of the 31 CMs.
- "p" represents one of the 5 renewable energy (RE) segments - Solar PV, CSP, Wind, BESS, or Electrolysers.
- "l" represents one of the 39 CETs across all RE segments.
- "k" represents one of the 9 time periods.
- L_{m_j,i_l,R_p,t_k} is the the requirement of CM "j" in CET "l" of a RE segment "p", in year "k".
- μ_{T,i_l,R_p,t_k} is the Market Share of CET "l" of a RE segment "p", in year "k".
- N_{T,R_p,t_k} is the generalized YoY capacity of a RE segment "p", in year "k".
- M_{m_j,i_l,R_p} is the material intensity of mineral "j" required in CET "l" of RE segment "p"

The second step is to calculate the YoY demand of each CM "j" across all the CETs under each RE segment "p" in time period "k". Equation 3 below gives the calculation. Figures 1-31 under section 4.1, are plotted using this equation.

$$\boldsymbol{Z_{m_j,R_p,t_k}} = \sum_{l=1}^{a} \boldsymbol{L_{m_j,i_l,R_p,t_k}} \text{ .... } \mathbf{(3)}$$

Where,

- Z_{m_j,R_p,t_k} is the YoY demand of CM "j" of a RE segment "p", in year "k".

Lastly, we calculate the total YoY demand of each CM "j" across all the RE segments in time period "k". Equation 4 below gives the calculation. Figures 32-37 under section 4.2, are plotted using this equation.

$$\boldsymbol{F_{m_j,t_k} = \sum_{p=1}^{b} Z_{m_j,R_p,t_k}} \text{ ……... (4)}$$

Where,

- F_{m_j,t_k} is the total YoY demand of critical mineral "j" across all RE segments in year "k".

This exercise has been extended to calculating the cumulative demand of each CM across all the RE segments by simply summing the YoY demand across the entire time-period (2025-2070). Figures 32-37 under section 4.2 plots the cumulative demand as well.

4. Results & Analysis

4.1. Year-on-Year Demand of Critical minerals in various RE segments

4.1.1. Solar PV & CSP

Table 1.1 [13-15] in the annexure presents mineral requirements for various Solar PV CETs. Crystalline Silicon PV types include Monocrystalline Silicon (mono-Si), Polycrystalline Silicon (poly-Si), and Heterojunction Silicon (HJT); Thin-Film PV technologies include Copper Indium Gallium Selenide (CIGS), and Cadmium Telluride (CdTe); and Perovskite technologies include perovskite/silicon tandem and Perovskite APT. CMs include Nickel, Tin, Copper, Silicon, Indium, Gallium, Selenium, Cadmium, Tellurium, Molybdenum, Tungsten, Graphite, Titanium, Lithium, and Germanium, highlighting the diverse material needs of the technologies. Table 1.2 [16] in the annexure provides data on the mineral requirements for two types of CSP CETs - Parabolic Troughs (a linear concentrating system) and Solar Power Towers (a point-focus system). The CMs include Copper, Molybdenum, Nickel, Titanium, Vanadium, and Niobium, offering a comprehensive look at the raw material demands of these CSP technologies.

In Figures 4.1 & 4.2, copper and silicon exhibit similar demand growth trends under both the BAU and NZ scenarios. This similarity primarily arises from their association with CETs that are projected to experience a decline in market share. Silicon is predominantly utilized in crystalline solar PV systems, whereas copper is required across crystalline, thin-film, and perovskite technologies. Despite copper's presence in thin-film and perovskite CETs, which are expected to gain market share, its overall demand trend closely follows that of silicon. This is because crystalline technologies, although declining, continue to dominate the market, thereby exerting significant influence on copper demand. Furthermore, the relatively low copper intensity in perovskite CETs limits their impact on its overall demand. Copper demand is also influenced by its role in both CSP technologies. Specifically, it is used in greater quantities in parabolic troughs, which have a larger but declining market share, contributing further to its demand trend.

In Figures 4.3-4.10, cadmium, tin, and tellurium display similar demand patterns due to their shared presence in the thin-film cadmium-telluride (CdTe) CET. A noticeable decline in their demand after 2065 occurs even though thin-film CETs gain market share. This is because CdTe's market share increases at a decreasing rate, stabilizing after 2060 under the BAU scenario and after 2055 under the NZ scenario. The earlier stabilization in NZ reflects the scenario's ambition and the limited adoption potential of CdTe, given cadmium's toxicity and geopolitical sensitivity.

Germanium exhibits a distinct demand trajectory. Under the BAU scenario, its demand fluctuates, rising initially before declining sharply to zero, reflecting its exclusive use in amorphous thin-film PV, a sub-technology projected to become obsolete post-2065 due to its low efficiency. In contrast, under the NZ scenario, in alignment with India's commitment to a diversified clean energy portfolio to achieve its 2070 Net Zero target, amorphous thin-film PV is assumed to experience a gradual decline rather than a complete phase-out. Consequently, Germanium demand under NZ continues to increase, albeit at a decreasing rate.

The remaining CMs, graphite, tungsten, gallium, indium, nickel, selenium, niobium, titanium, molybdenum, vanadium, and lithium, exhibit broadly similar demand trends characterized by similar fluctuations. Except for vanadium and niobium, which are used exclusively in CSP, these minerals are primarily associated with solar PV CETs such as thin-film and perovskite technologies that exhibit growing market shares. Notably, graphite demand emerges only after 2040, aligning with the expected market entry of Perovskite APT around that time [8]. Among the CSP-associated minerals, nickel and titanium are required in parabolic troughs, which, despite their declining dominance, still represent a major share of CSP capacity. Titanium is used solely in this CET, whereas nickel is present in both CSP technologies, though its mineral intensity in parabolic troughs is roughly half that in solar power towers, which have a smaller but increasing market share. In contrast, molybdenum is also present in both CSP CETs, but its intensity in parabolic troughs is nearly four times that of solar power towers, leading to more pronounced demand fluctuations. Vanadium, required in minimal quantities across both CSP CETs, shows limited fluctuation, whereas niobium, used solely in solar power towers, exhibits a relatively stable yet variable trend. Lithium and vanadium are the only two minerals whose demand is represented in tonnes rather than kilo tonnes, owing to their comparatively low overall demand.

Overall, while the diversity of CETs and their respective mineral intensities shape the individual demand trajectories of these CMs, the general trend remains upward. The demand for CMs required in the solar energy sector is primarily driven by the market share and diversity of CETs, reflecting the technological mix and transition pathways under each scenario.

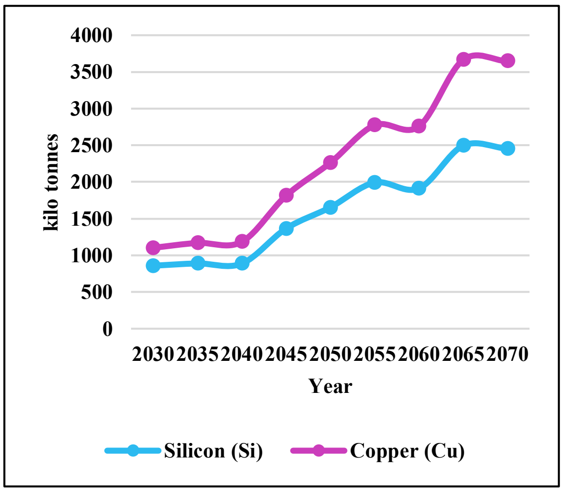

Figure 4.1: Requirement of critical minerals for Solar under BAU

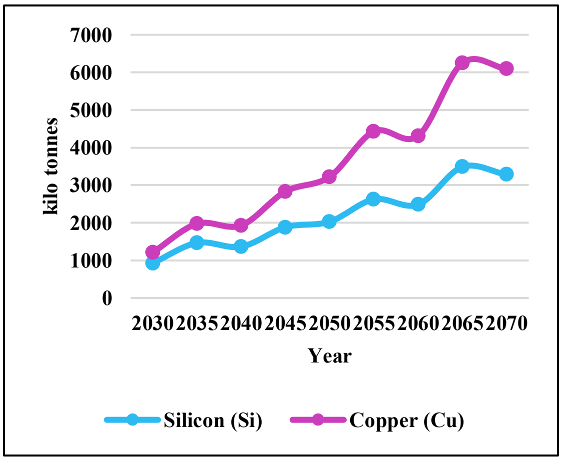

Figure 4.2: Requirement of critical minerals for Solar under NZ

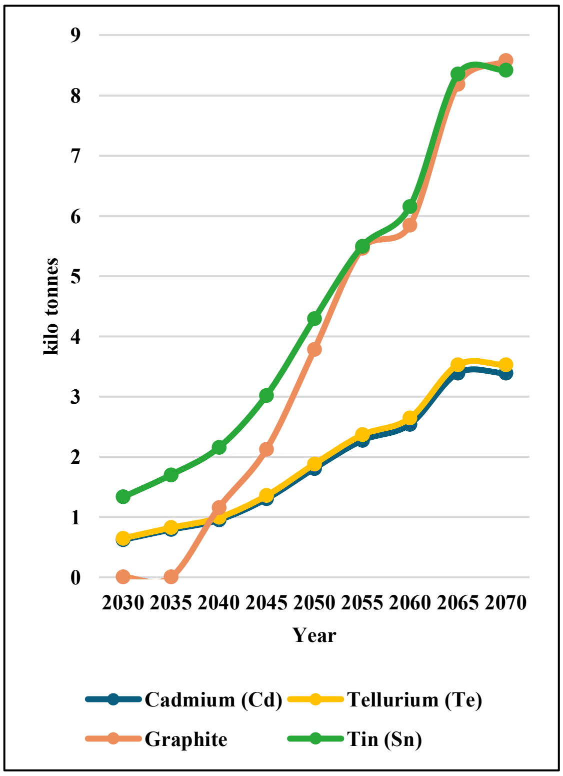

Figure 4.3: Requirement of critical minerals for Solar under BAU

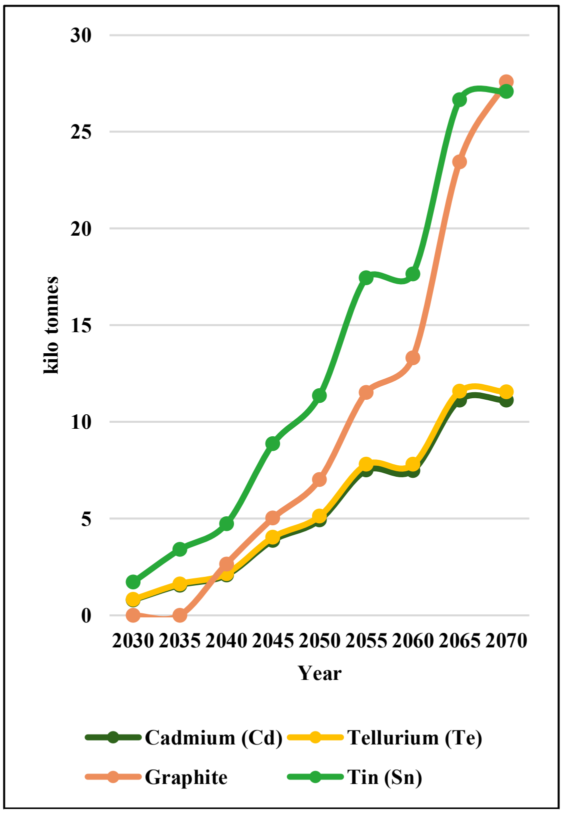

Figure 4.4: Requirement of critical minerals for Solar under NZ

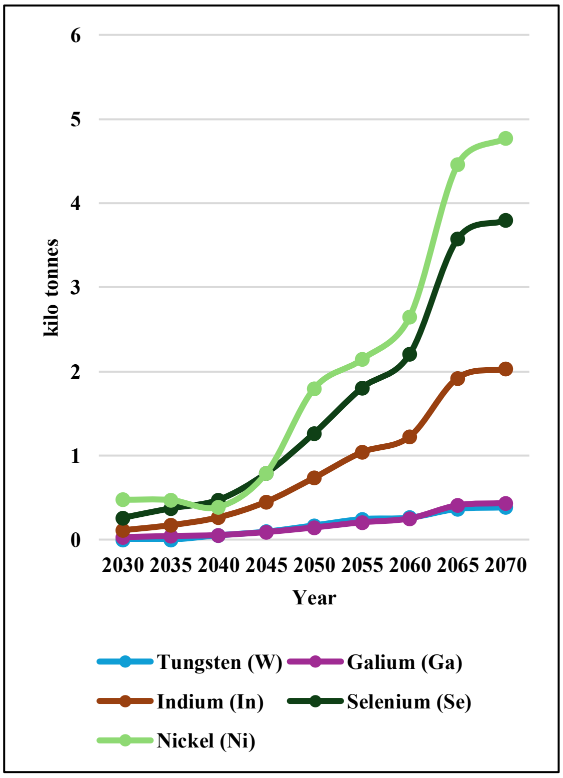

Figure 4.5: Requirement of critical minerals for Solar under BAU

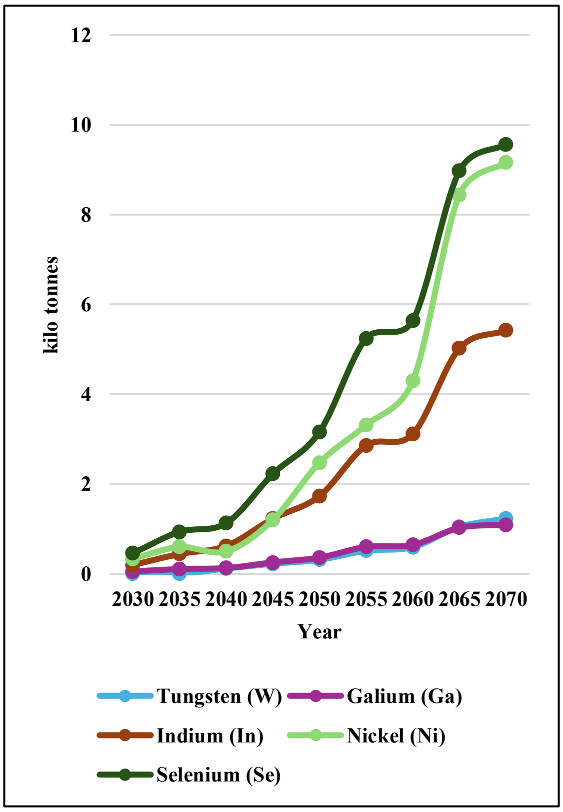

Figure 4.6: Requirement of critical minerals for Solar under NZ

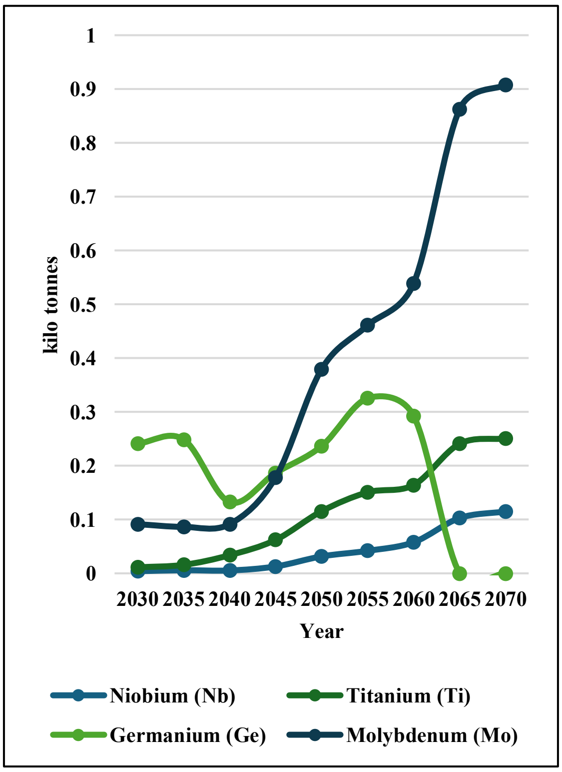

Figure 4.7: Requirement of critical minerals for Solar under BAU

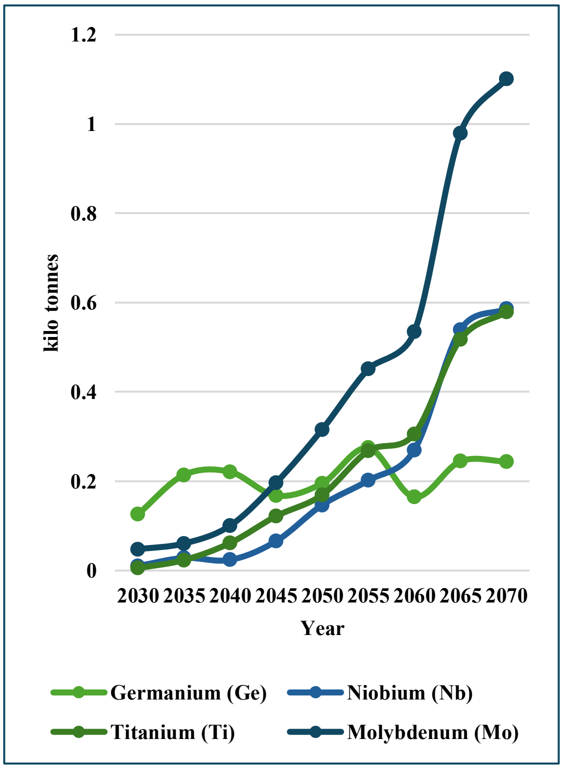

Figure 4.8: Requirement of critical minerals for Solar under NZ

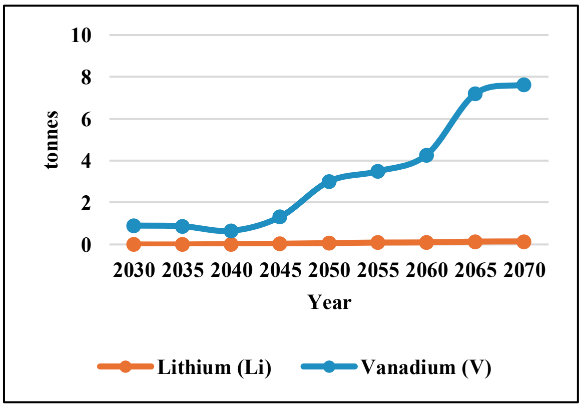

Figure 4.9: Requirement of critical minerals for Solar under BAU

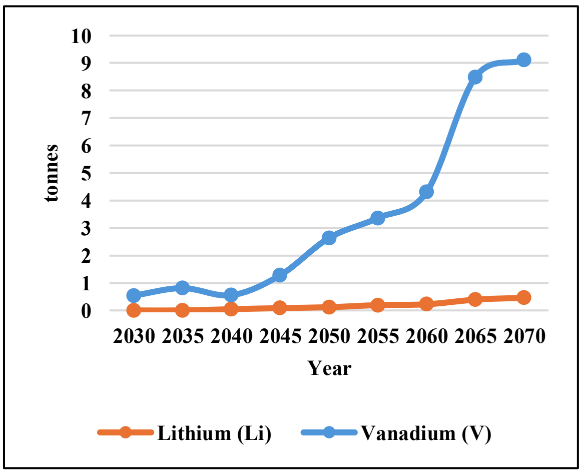

Figure 4.10: Requirement of critical minerals for Solar under NZ

4.1.2. Wind

Table 1.3 [17 & 18] in the annexure outlines mineral requirements for different Wind Technology types, categorized by onshore and offshore wind turbine systems, specifically focusing on direct-drive and gearbox technologies. CMs include Copper, Molybdenum, Neodymium, Nickel, Dysprosium, Praseodymium, Terbium, and Yttrium.

Figures 4.11-4.17 illustrate the demand growth trends of CMs required in CETs for both onshore and offshore wind energy systems. Overall, the demand trajectories under both scenarios exhibit broadly similar patterns. In each case, the demand for CMs grows linearly up to 2040, followed by a phase of increasing growth at a decreasing rate until 2055 under BAU and 2060 under NZ, and subsequently transitions into an exponential growth phase beyond 2060. This pattern directly corresponds to the projected YoY capacity additions in wind energy, which are expected to increase rapidly until 2040, moderate between 2040 and 2060, and accelerate again, potentially exponentially, after 2060.

A notable exception is yttrium, whose demand behaviour diverges from that of other minerals. Yttrium is exclusively required in the direct-drive high-temperature superconductor (DD-HTS) CET of offshore wind and therefore appears only under the BAU scenario. In the NZ scenario, the DD-HTS technology is replaced by more advanced CETs, eliminating yttrium's market presence. Under BAU, yttrium's demand trend is characterized by noticeable fluctuations: it increases rapidly until 2040, grows at a decreasing rate until around 2065, and then declines thereafter. This behaviour can be attributed to two main factors: first, its extremely low mineral intensity in DD-HTS technology, and second, the stabilization of DD-HTS's market share at approximately 17% beyond 2060, which constrains further demand growth. Across both onshore and offshore wind technologies, copper records the highest overall demand, followed by nickel. Other critical minerals with significant contributions include dysprosium, molybdenum, neodymium, praseodymium, and terbium. Among these, copper and molybdenum are utilized across all CETs within both onshore and offshore segments, emphasizing their essential role in wind energy infrastructure.

In summary, the demand growth of critical minerals in the wind energy sector is predominantly determined by the rate of capacity additions. While technological differentiation, particularly in offshore systems, modulates the demand for specific minerals such as yttrium, overall capacity expansion remains the key driver of CM demand under both the BAU and NZ scenarios.

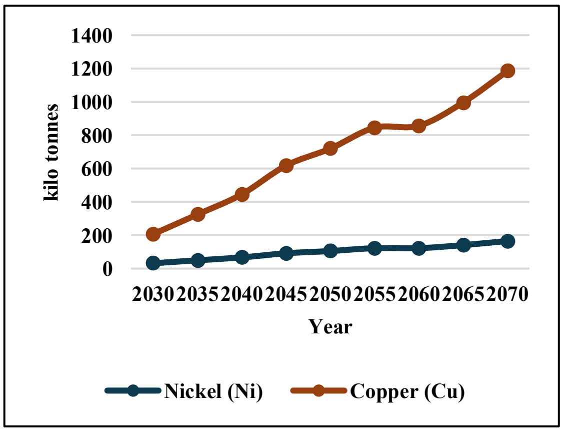

Figure 4.11: Requirement of critical minerals for Wind under BAU

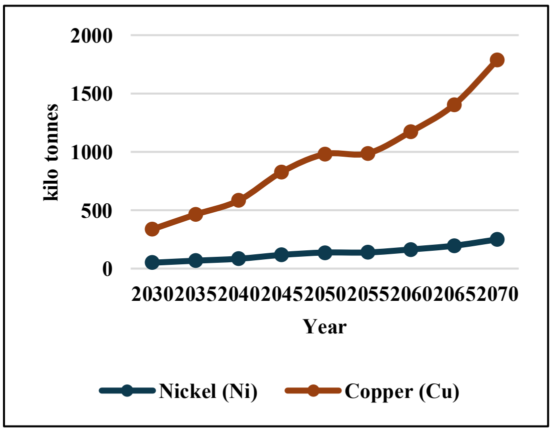

Figure 4.12: Requirement of critical minerals for Wind under NZ

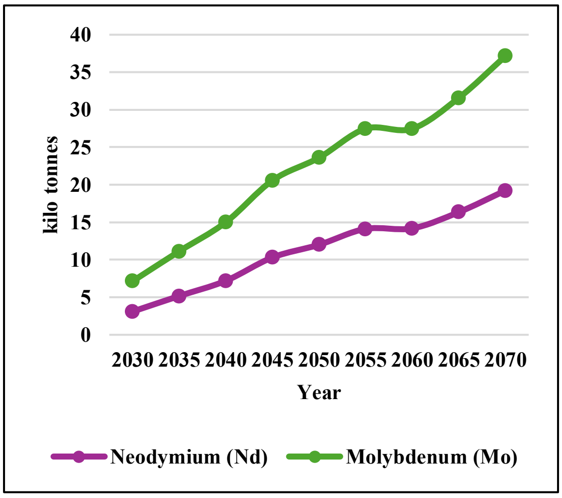

Figure 4.13: Requirement of critical minerals for Wind under BAU

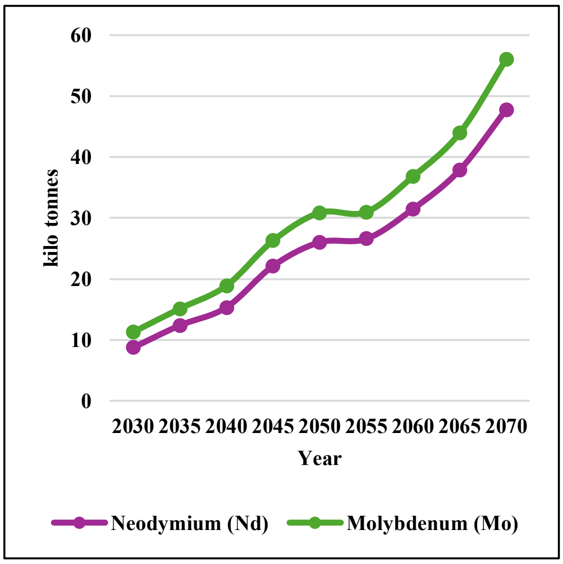

Figure 4.14: Requirement of critical minerals for Wind under NZ

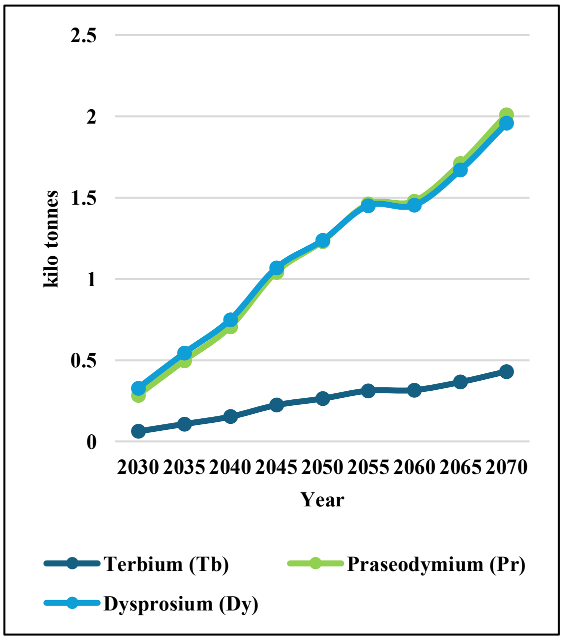

Figure 4.15: Requirement of critical minerals for Wind under BAU

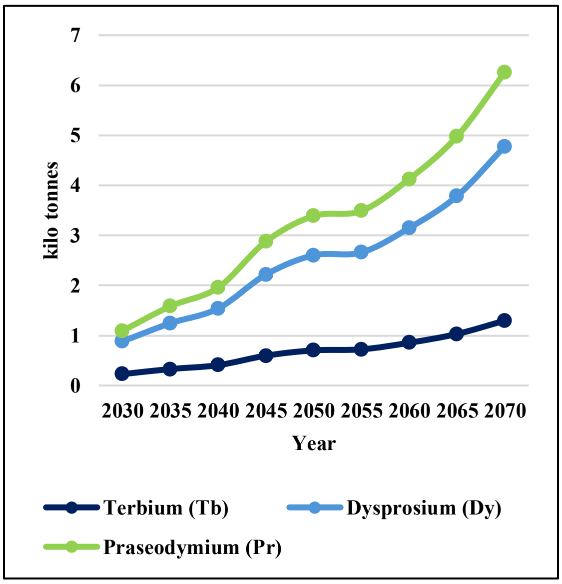

Figure 4.16: Requirement of critical minerals for Wind under NZ

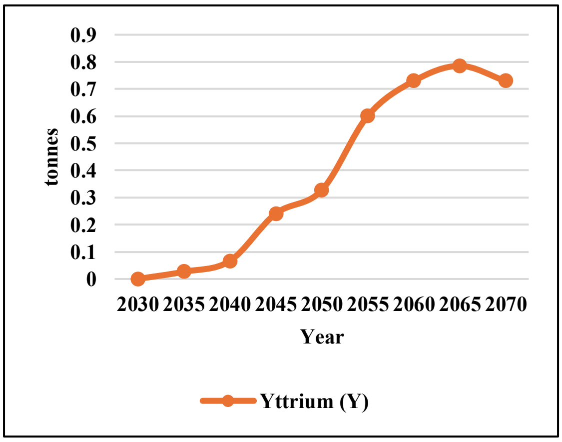

Figure 4.17: Requirement of critical minerals for Wind under NZ

4.1.3. Stationary Battery Energy Storage Systems

Table 1.4 [10,13, 19-24] in the annexure provides a comparative overview of various BESS CETs, highlighting the CM requirements for each. Each technology is listed with its category abbreviation alongside the quantities of specific minerals needed in tonnes per gigawatt hour (t/GWh). The CMs tracked include Graphite, Lithium, Cobalt, Nickel, Copper, Vanadium, Titanium and Phosphorous, offering a comprehensive look at the raw material demands of these storage technologies. The technologies include Lithium-ion batteries, Sodium-ion batteries, Vanadium Redox Flow Battery (VRFB), Polysulfide Bromide, Sodium-Sulphur, Lithium-Sulphur batteries, and Zinc-Bromine. It is to be noted that Polysulfide Bromide, Sodium-Sulphur and Zinc-Bromine technologies have no CMs and hence are outside of the scope of this study.

Figures 4.18-4.21 illustrate the demand growth trends of CMs required in CETs for BESS under the BAU and NZ scenarios. Although the overall demand trajectories differ between the two scenarios, the CMs within each scenario exhibit internally consistent patterns.

Under the BAU scenario, CM demand increases at an accelerating rate until 2035, followed by a decline up to 2040. Between 2040 and 2065, demand rises again with minimal fluctuations, after which it declines beyond 2065. This general pattern is observed across most CMs. In contrast, under the NZ scenario, demand declines from 2030 to 2035, then rises at an increasing rate until 2045, grows at a decreasing rate until 2050, falls again up to 2055, and finally increases beyond 2055 with limited fluctuations. These variations in trend across scenarios primarily reflect differences in projected capacity additions for stationary BESS deployment. Graphite records the highest overall demand, primarily due to its high mineral intensity in lithium iron phosphate (LFP) systems, which dominates BESS market share during much of the projection period. This is followed by copper, phosphorus, and vanadium. Copper’s relatively high demand is attributed to its use in VRFB, LFP), and lithium nickel manganese cobalt oxide (LNMC) systems. However, since LNMC technologies are projected to lose market presence beyond 2030, primarily due to the phase-out of cobalt, copper’s demand predominantly originates from VRFB, which holds a small but rising share, and from LFP, which has a large but declining share. Cobalt exhibits the lowest demand among all CMs because the CETs in which it is used (primarily LNMCs) are phased out by 2030 due to cobalt’s toxicity and supply risks. Nevertheless, cobalt maintains a modest demand through its presence in sodium nickel manganese cobalt oxide (NaNMC), which shows an increasing market share. Consequently, cobalt’s demand profile is smoother and less volatile than that of other CMs. Titanium follows a similar trend, being used exclusively in lithium titanate oxide (LTO), a CET with a steadily increasing market share. Nickel and lithium are required in multiple CETs, six and seven respectively, three of which are LNMCs that are phased out by 2035. Among the remaining CETs, all lithium-containing technologies (except LFP) display rising market shares, supporting continued lithium demand growth.

In summary, the demand growth of critical minerals in stationary BESS is governed by three primary factors: the market share of specific CETs, the rate of capacity additions, and the number of CETs utilizing each mineral. Together, these variables determine the magnitude and volatility of CM demand across both the BAU and NZ scenarios.

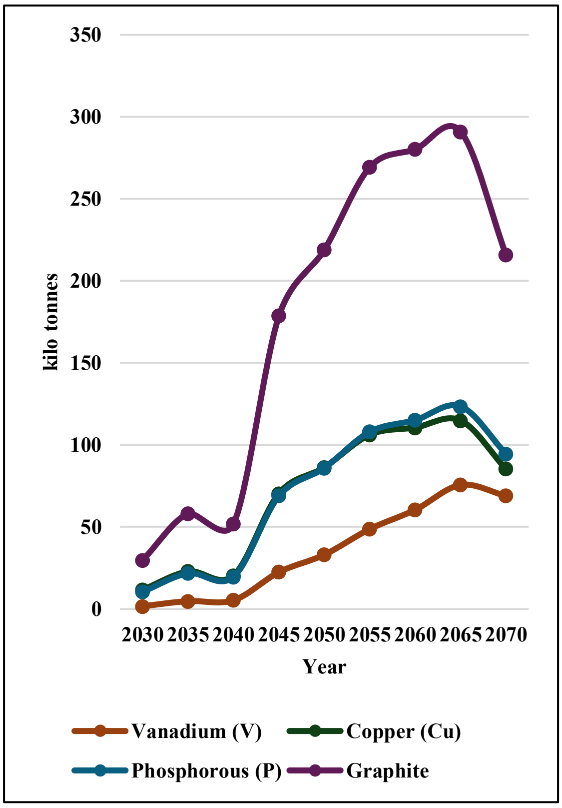

Figure 4.18: Requirement of critical minerals for BESS under BAU

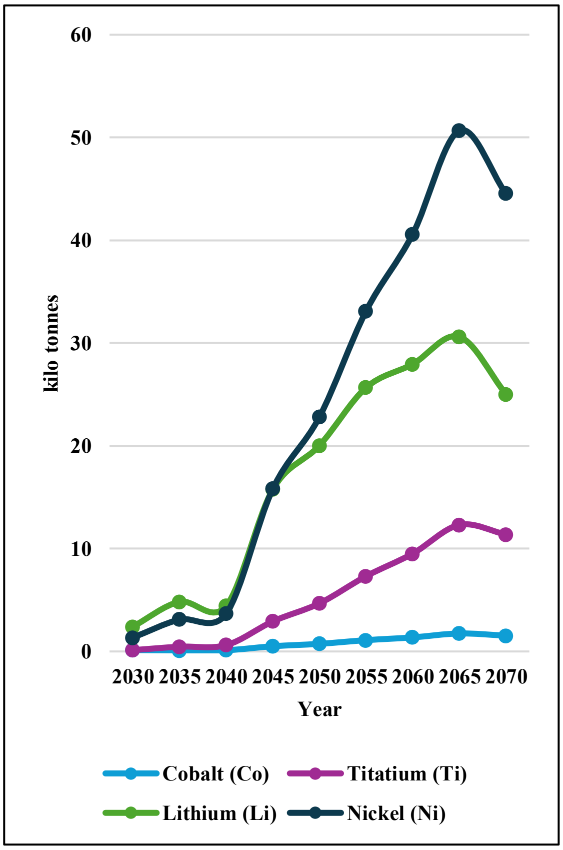

Figure 4.20: Requirement of critical minerals for BESS under BAU

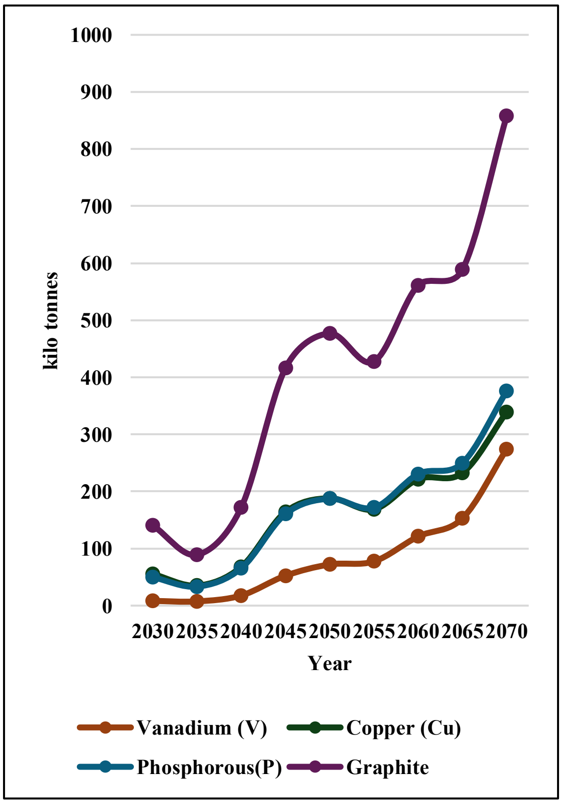

Figure 4.19: Requirement of critical minerals for BESS under NZ

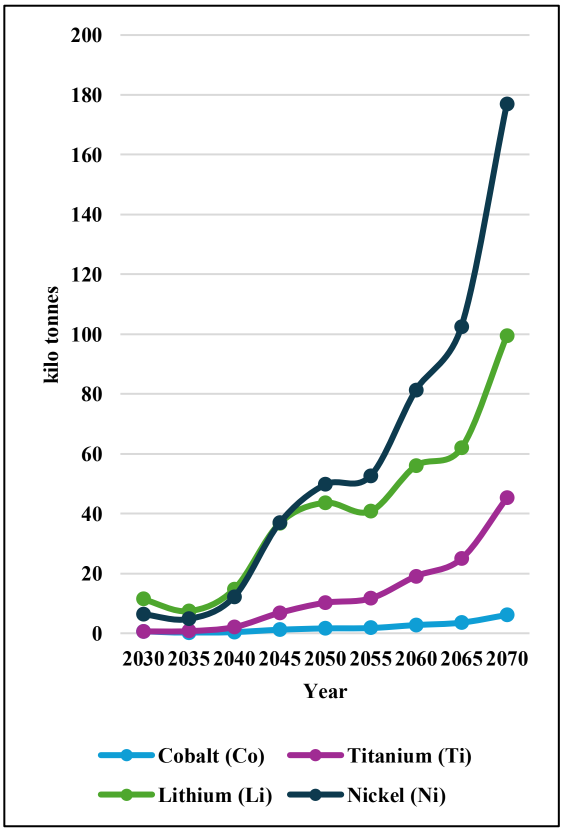

Figure 4.21: Requirement of critical minerals for BESS under NZ

4.1.4. Green Hydrogen Electrolyser

Table 1.5 [6,7,25-27] in the annexure outlines that the CMs required for green hydrogen production vary across different electrolyser technologies. Alkaline Electrolysers (AEL) primarily rely on copper, zirconium, nickel, graphite, and cobalt. Proton Exchange Membrane Electrolysers (PEMEL) utilize copper, graphite, iridium, platinum-group metals, and silicon. Solid Oxide Electrolysis (SOEL) requires a diverse range of CMs, including Copper, Zirconium, Nickel, Silicon, Titanium, Lanthanum, Strontium, Gadolinium, Cerium, and Yttrium.

Figures 3.22–3.31 depict the demand growth trends of CMs required in CETs used in electrolysers for green hydrogen production. Under both the BAU and NZ scenarios, the overall demand trajectories of these CMs exhibit similar cyclical patterns, though the magnitude of fluctuations varies across minerals.

In the BAU scenario, CM demand declines between 2030 and 2035, rises until 2040, falls again until 2045, increases to 2050, declines once more up to 2055, and then grows beyond 2055. While all CMs follow this general pattern, certain minerals including nickel, copper, graphite, cobalt, and zirconium, exhibit sharper and more pronounced fluctuations compared to iridium, platinum, titanium, silicon, lanthanum, yttrium, strontium, cerium, and gadolinium, which display relatively smoother demand curves. This divergence in volatility can be attributed to differences in mineral utilization across CETs. The minerals with sharper fluctuations are required in high quantities in AEL, which hold a dominant (until around 2040) but declining market share. Although nickel, copper, graphite, and zirconium are also used in PEMEL and SOEL, technologies with increasing market shares, their lower mineral intensities in these CETs limit their influence on overall demand trends. Conversely, the minerals exhibiting flatter trends are predominantly used in PEMEL and SOEL technologies, whose market shares are steadily increasing, thereby producing smoother growth trajectories.

Under the NZ scenario, a broadly similar pattern is observed: demand decreases between 2030 and 2035, increases up to 2050, declines again until 2055, and rises thereafter. As in the BAU scenario, nickel, copper, graphite, cobalt, and zirconium display more pronounced demand fluctuations than iridium, platinum, titanium, silicon, lanthanum, yttrium, strontium, cerium, and gadolinium. The underlying reason remains consistent, the minerals with sharper fluctuations are concentrated in CETs with declining market dominance (primarily AEL), whereas those with smoother demand trends are associated with emerging technologies (PEMEL and SOEL) that gain prominence over time.

Nickel exhibits the highest demand, followed by copper, notably due to its high mineral intensity. Overall, the demand growth trajectories of critical minerals in electrolysers are governed primarily by two determinants: (1) the rate of capacity additions under each scenario and (2) the evolving market shares of individual CETs. Together, these factors shape both the magnitude and variability of mineral demand in the green hydrogen sector.

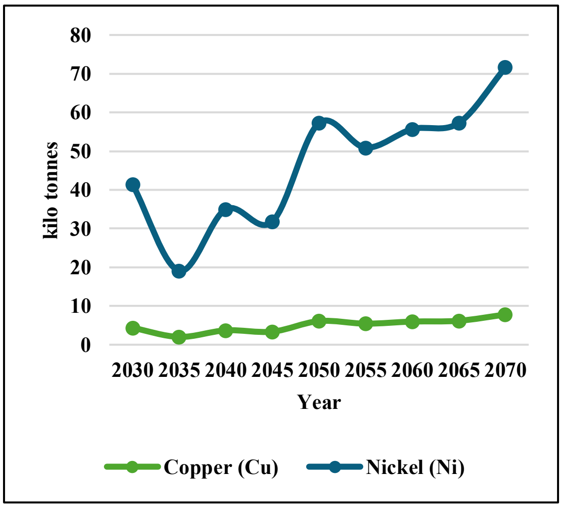

Figure 4.22: Requirement of critical minerals for Green Hydrogen Electrolysers under BAU

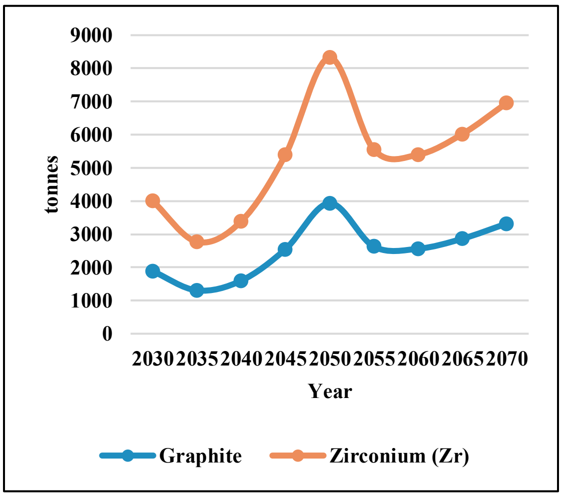

Figure 4.25: Requirement of critical minerals for Green Hydrogen Electrolysers under NZ

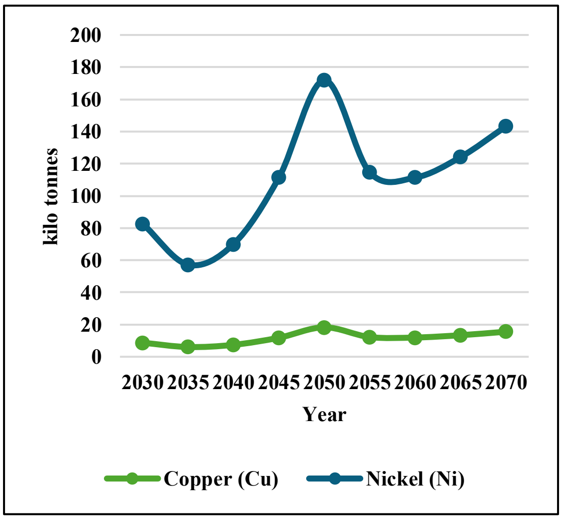

Figure 4.24: Requirement of critical minerals for Green Hydrogen Electrolysers under NZ

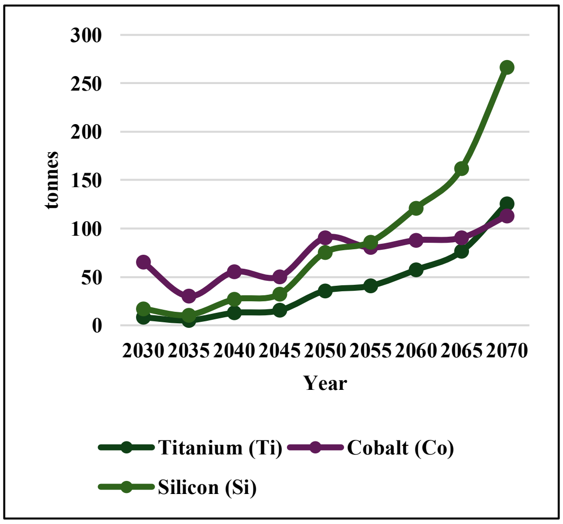

Figure 4.26: Requirement of critical minerals for Green Hydrogen Electrolysers under BAU

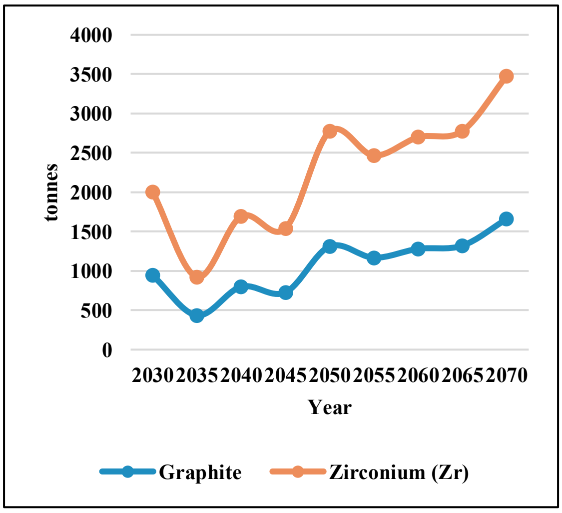

Figure 4.24: Requirement of critical minerals for Green Hydrogen Electrolysers under BAU

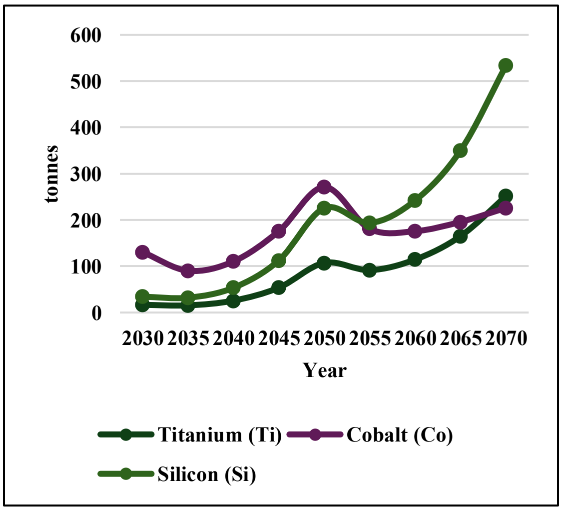

Figure 4.27: Requirement of critical minerals for Green Hydrogen Electrolysers under NZ

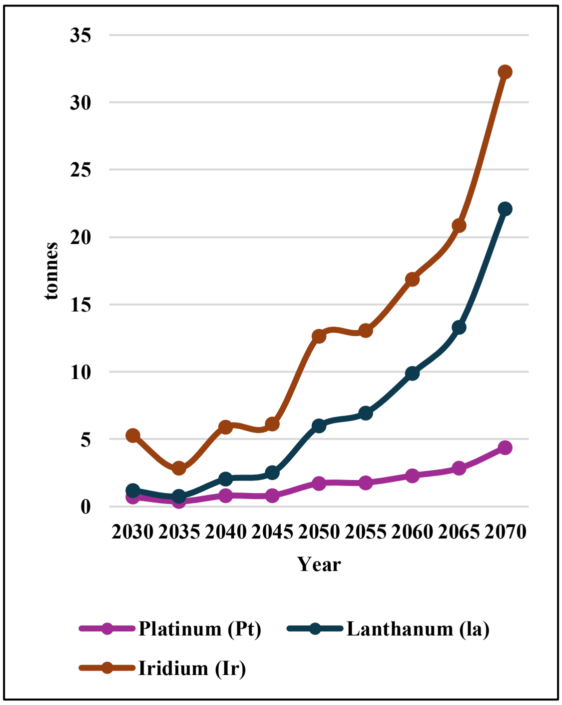

Figure 4.28: Requirement of critical minerals for Green Hydrogen Electrolysers under BAU

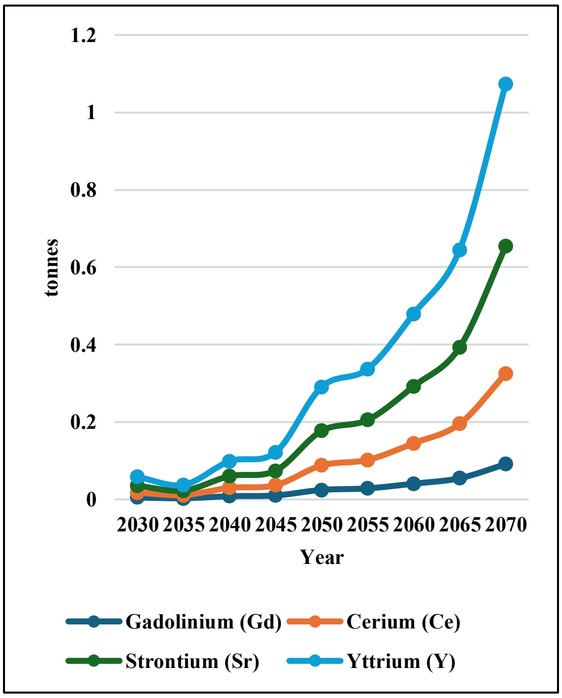

Figure 4.30: Requirement of critical minerals for Green Hydrogen Electrolysers under BAU

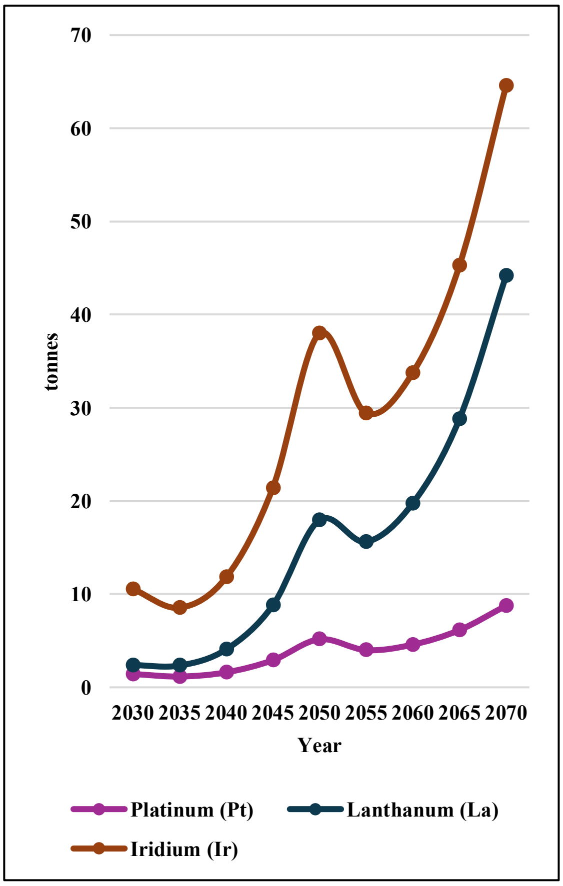

Figure 4.29: Requirement of critical minerals for Green Hydrogen Electrolysers under NZ

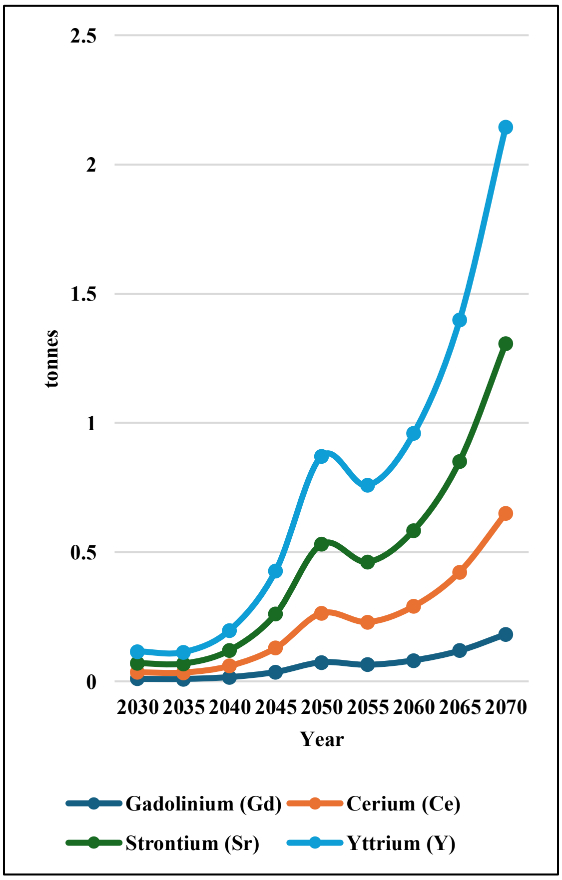

Figure 4.31: Requirement of critical minerals for Green Hydrogen Electrolysers under NZ

4.2. Total Year-on-Year Demand and Cumulative Demand of Critical Minerals for Manufacture of Clean Energy Technologies

In figure 4.32-4.37 the X-axis represents the YoY as well as the cumulative demand for critical minerals over the period from 2030 to 2070. Each segment of each stacked bar illustrates the YoY demand for CMs within a specific time period, showing how the demand evolves over the years. Whereas the length of each stacked bar represents the cumulative demand for CMs until 2070. Cumulative demand, under BAU scenario as well as NZ scenario, among the CMs, Copper (27.2 million tonnes under BAU and 42.3 million tonnes under NZ) and Nickel (1.5 million tonnes under BAU and 2.7 million tonnes under NZ) stand out for both their high cumulative demand and diverse applications across CETs across RE segments. Silicon records the second highest cumulative demand (14.5 million tonnes under BAU and 19.5 million tonnes under NZ) after copper, owing to its pivotal role in Solar PV and electrolysers. Graphite records the third highest cumulative demand (1.6 million tonnes under BAU and 3.8 million tonnes under NZ) due to its important role in BESS, especially in battery anodes and a small share in graphene form for emerging perovskite solar cells.

Figures 4.32 and 4.33 are presented in kilo tonnes (high-demand) to reflect the high demand of the CMs shown. Figures 4.34 and 4.35 are given in tonnes (moderate-demand), while Figures 4.36 and 4.37 are in kilo grams (low-demand) due to the significantly lower demand of the CMs represented.

Figures 4.32 and 4.33 illustrate that under the BAU scenario, molybdenum exhibits higher demand compared to lithium, whereas under the NZ scenario, lithium demand surpasses that of molybdenum. This reversal can be attributed primarily to the higher YoY capacity additions projected under the NZ scenario, particularly within the stationary BESS sector.

Moreover, these figures indicate that under the NZ scenario, tin and cadmium appear among the high-demand CMs, whereas they are absent from the corresponding list under BAU, where they are classified as moderately demanded minerals. The rise in tin demand under NZ can be explained by both the increase in YoY capacity additions and the expansion in the market share of solar PV CETs, particularly CdTe and perovskite technologies, relative to the BAU scenario. Similarly, cadmium demand increases under NZ due to the combined effects of higher capacity additions and the growing market share of CdTe technologies.

Figures 4.34 and 4.35 illustrate notable differences in the demand trends of several CMs under the BAU and NZ scenarios. Under the BAU scenario, zirconium exhibits higher demand than tellurium, whereas under the NZ scenario, tellurium demand surpasses that of zirconium. This reversal can be primarily attributed to the increasing market share of CdTe technologies, which require tellurium, and the simultaneous decline in the market share of AEL, the major consumer of zirconium. Although zirconium is also utilized in SOEL, its mineral intensity in SOEL is relatively low, resulting in a negligible contribution to overall zirconium demand.

Under the BAU scenario, dysprosium demand exceeds that of praseodymium, but under the NZ scenario, the relationship reverses. Both minerals are used exclusively in wind CETs. In onshore wind systems, dysprosium is required in four of five CETs, while praseodymium is used in only two. In offshore wind, dysprosium is used in three of four CETs and praseodymium in two. Despite being used in fewer CETs, the total mineral intensity of praseodymium across both onshore and offshore systems exceeds that of dysprosium. In onshore wind, both minerals are required in GB-HS-PMSG and DD-PMSG, which follow similar growth trajectories under both scenarios; thus, these CETs do not explain the observed reversal in demand. However, dysprosium is additionally used in GB-DFIG and GB-SCIG. Under the BAU scenario, the market share of GB-DFIG declines moderately from 25% to 6%, and that of GB-SCIG from 2% to 0.7%. Under the NZ scenario, both CETs experience steeper declines, GB-DFIG from 8% to 0% and GB-SCIG from 1.6% to 0%. This difference helps explain the higher dysprosium demand under BAU (when these CETs still hold a meaningful share) and the higher praseodymium demand under NZ (when these CETs become nearly obsolete). Another reason is that in offshore wind, under BAU, dysprosium is used in GB-SCIG, a technology not requiring praseodymium, which maintains a relatively high but declining market share, from 57% to 45%. Under NZ, the same CET's share drops sharply from 6% to 3%. Furthermore, in offshore wind, both praseodymium and dysprosium are required in DD-PMSG and GB-MS-PMG. Under BAU, these two CETs grow moderately, but under NZ, DD-PMSG becomes the dominant technology, increasing its market share from 75% to 88%, while GB-MS-PMG declines from 18% to 9%. The strong expansion of DD-PMSG, combined with praseodymium's higher mineral intensity, largely explains its higher demand under NZ.

In these figures, another contrast is observed between cobalt and indium. Under the BAU scenario, cobalt demand exceeds that of indium, whereas under NZ, indium demand becomes higher. Indium is used exclusively in solar PV, specifically in thin-film copper indium gallium selenide (CIGS) technology, while cobalt is required in both BESS and hydrogen electrolysers. Despite cobalt's higher mineral intensity (in tonnes per GW), its overall demand declines due to shifts in CET market shares. In BESS, cobalt is used in all LNMC chemistries, whose market share phases out by 2035, and in sodium nickel manganese cobalt oxide (NaNMC), which has a small but increasing share. In electrolysers, cobalt is required only in AEL, which maintains a dominant share until 2040 before declining. Conversely, indium demand increases under NZ because CIGS technology gains market share relative to BAU, coupled with higher YoY capacity additions in solar PV deployment. Thus, cobalt's dominance under BAU and indium's under NZ reflect these structural and technological transitions.

Finally, in these figures, the relative demand rankings of germanium, gallium, tungsten, and niobium also shift between the two scenarios. Under BAU, the descending order of demand is germanium, gallium, tungsten, and niobium; under NZ, it becomes gallium, tungsten, niobium, and germanium. All four minerals are used exclusively in solar PV technologies, except niobium, which is utilized only in CSP. This reordering is primarily driven by differences in mineral intensities and capacity additions across the two scenarios.

Figures 4.36 and 4.37 exhibit the same descending order of CMs under both scenarios, indicating no observable anomaly. These CMs are exclusively utilized in electrolyser technologies, and their demand patterns directly reflect their respective mineral intensities.

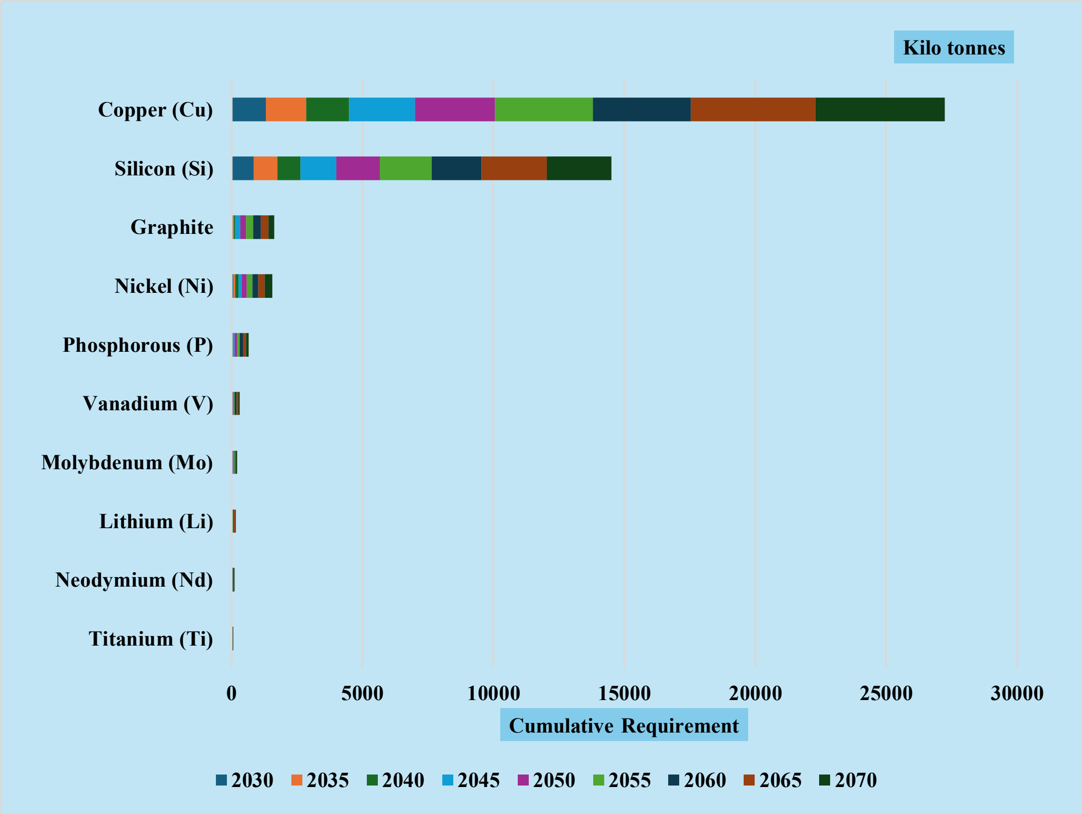

Figure 4.32: Total YoY & Cumulative demand for critical minerals over the period from 2030 to 2070 under

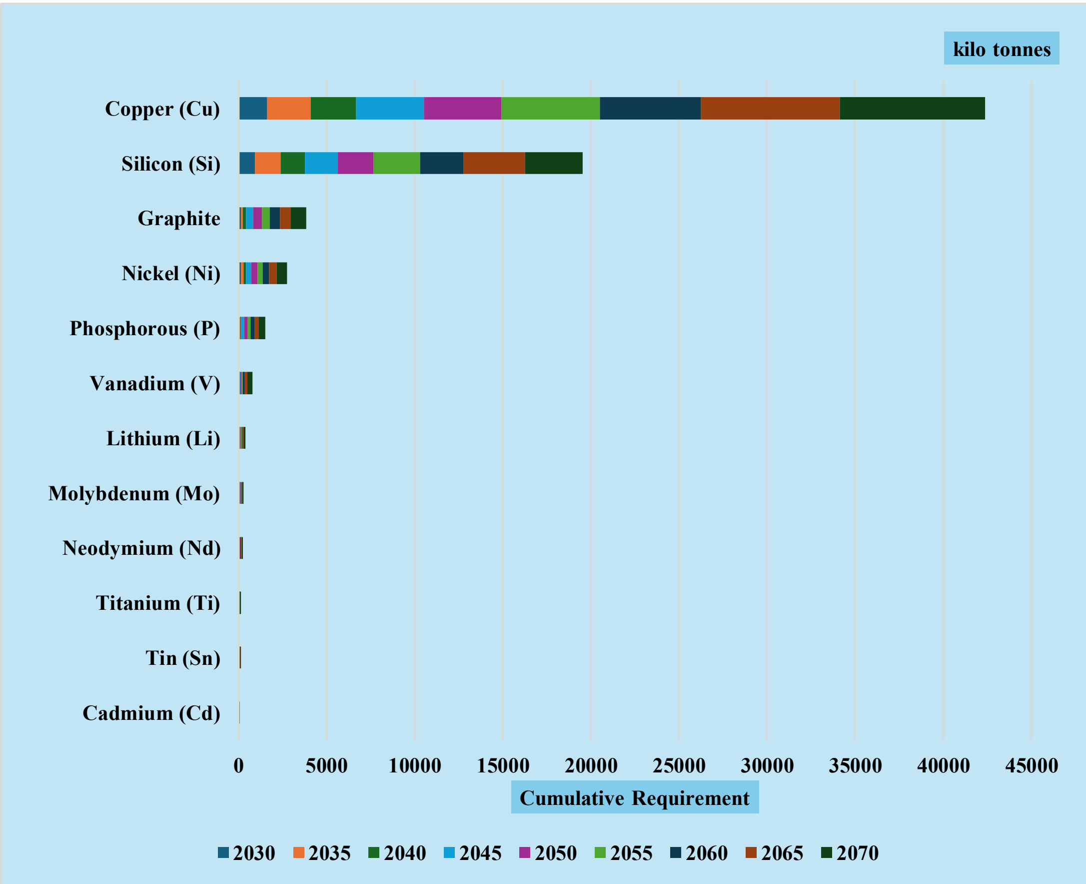

Figure 4.33: Total YoY & Cumulative demand for critical minerals over the period from 2030 to 2070 under NZ

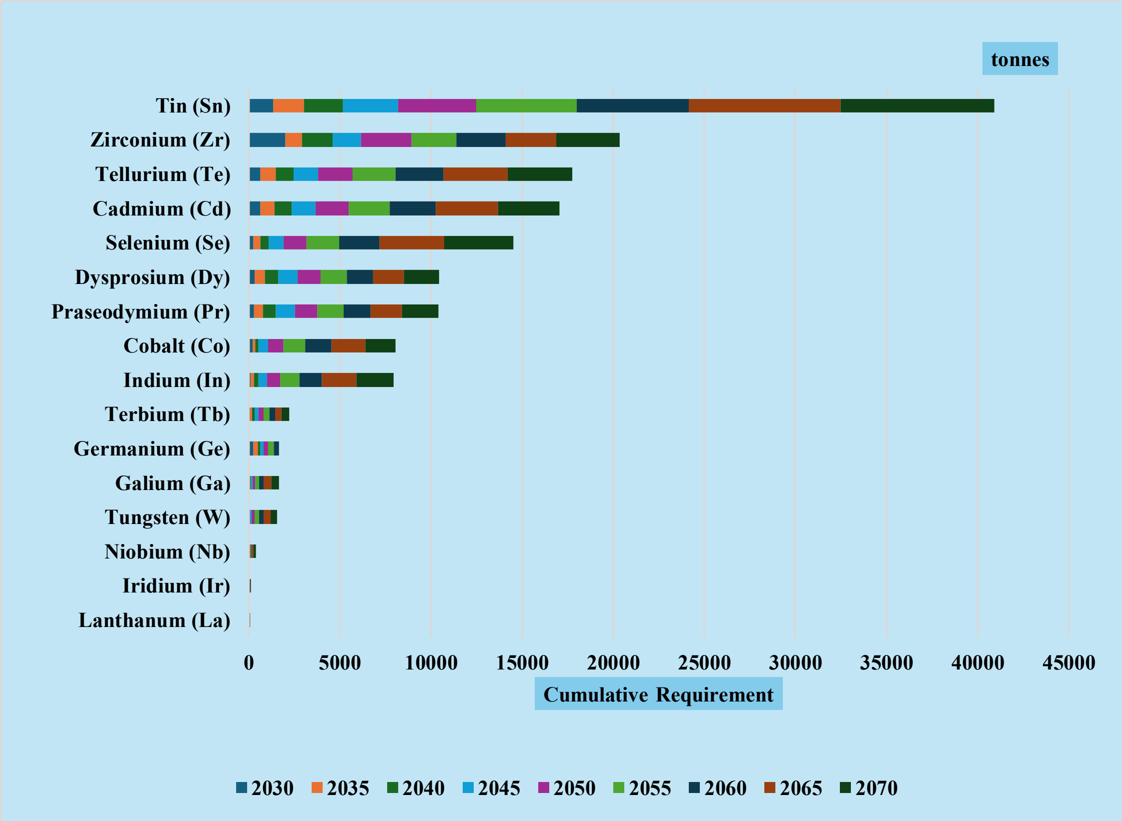

Figure 4.34: Total YoY & Cumulative demand for critical minerals over the period from 2030 to 2070 under BAU

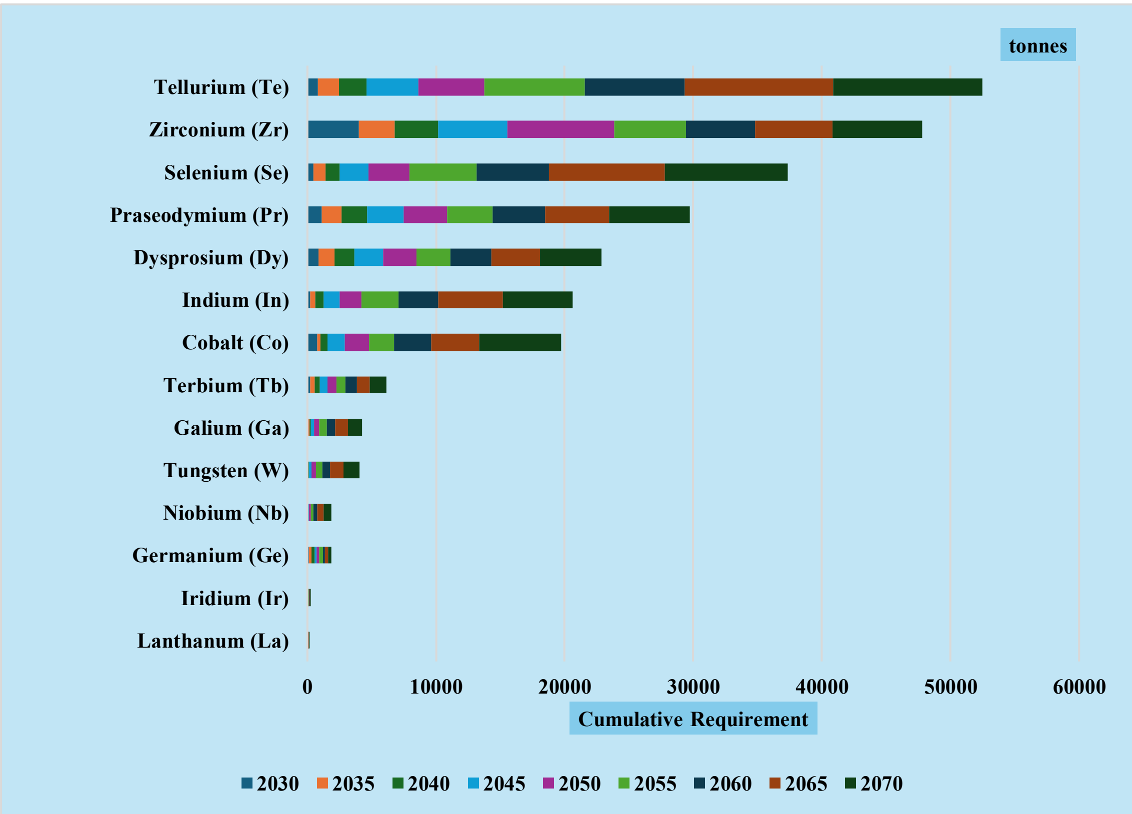

Figure 4.35: Total YoY & Cumulative demand for critical minerals over the period from 2030 to 2070 under NZ

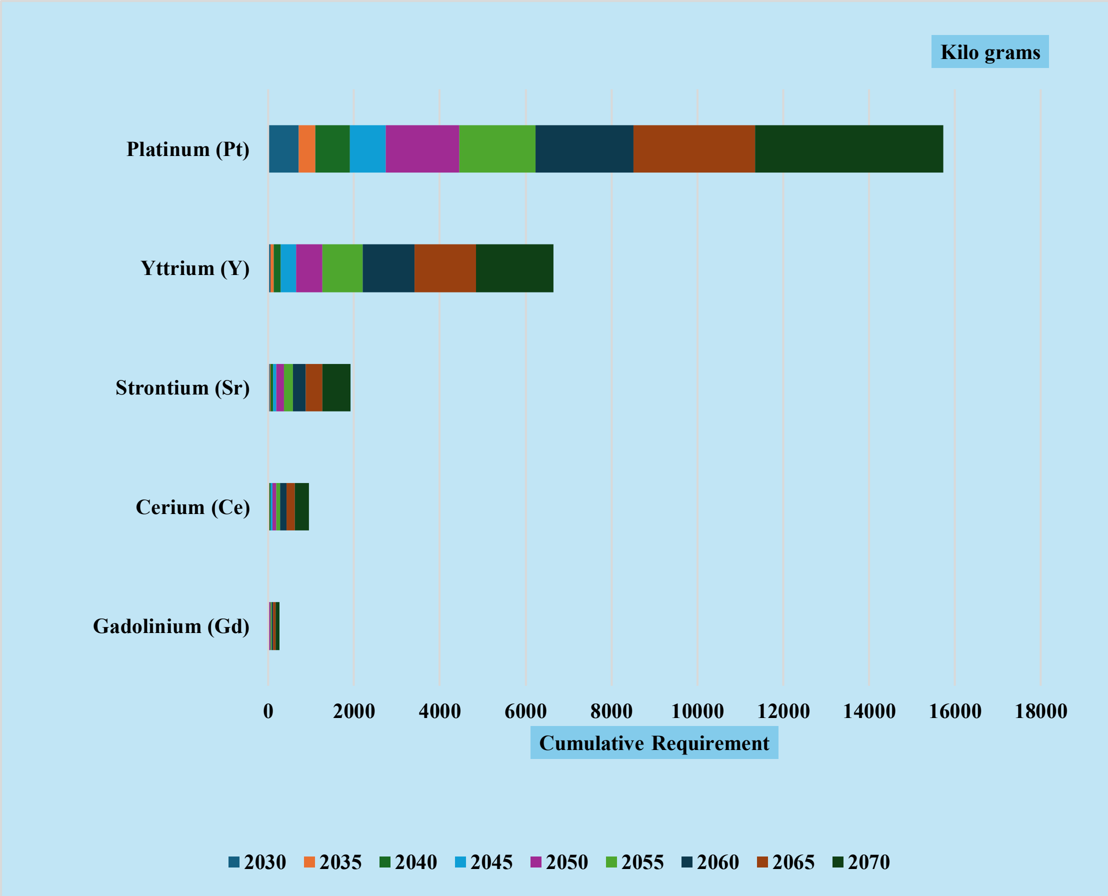

Figure 4.36: Total YoY & Cumulative demand for critical minerals over the period from 2030 to 2070 under BAU

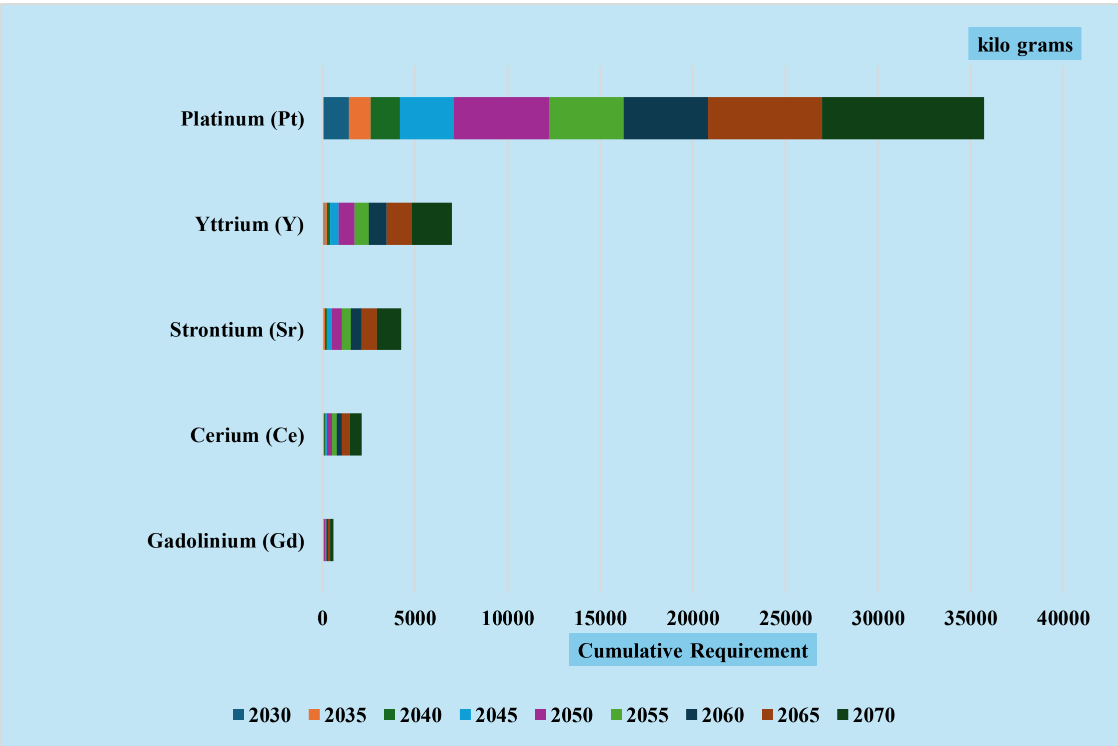

Figure 4.37: Total YoY & Cumulative demand for critical minerals over the period from 2030 to 2070 under NZ

5. Discussion

The results and analysis of this study indicate that Copper, Silicon, Graphite, Nickel, Phosphorous, Vanadium, Lithium, and Rare Earth Elements (REEs) will experience the highest cumulative demand. A 2024 policy brief by IEEFA identifies Copper, Cobalt, Graphite, Lithium, and Nickel as India's five most important CMs, in terms of demand and supply risk, for the clean energy transition [9]. While Copper, Graphite, Lithium and Nickel are one of the the top CMs in terms of demand and supply risk, this study has succeeded in significantly reducing the demand and hence the supply risk of Cobalt. Under BAU, the YoY demand growth of copper is expected to increase 4 times, Nickel 4 times, Graphite 7 times, and Lithium 10 times. Whereas under NZ the YoY demand growth of copper is expected to increase 5 times, Nickel 4 times, Graphite nearly 6 times, and Lithium 9 times.

These demand patterns are influenced by several factors. Copper and Nickel are required in large quantities across all renewable energy (RE) segments. REEs are required in large quantities in wind energy, while Graphite, Vanadium, and Lithium are particularly essential for BESS [10].

Crystalline silicon (c-Si) solar cells, including monocrystalline and polycrystalline types, initially, dominate the global solar market, holding over 80% of the share. Monocrystalline silicon panels, with efficiencies reaching up to 26%, are favored for their high performance, while polycrystalline panels, with efficiencies around 21%, offer a more cost-effective alternative. Thin-film solar technologies, such as CdTe, CIGS, and Amorphous Silicon (a-Si), collectively account for around 20% of the market eventually. These technologies provide advantages in flexibility and lower manufacturing costs, with efficiencies ranging from 12% for a-Si to over 21% for CdTe and CIGS. Emerging third-generation solar technologies, like Perovskite cells remain in the research phase, with efficiencies typically below 20%. While they currently have a negligible market share, ongoing advancements in materials and efficiency improvements may enhance their competitiveness in the future, leading to an initially low demand for Nickel and Graphite, which is projected to increase over time [11]. This study has compared the material demands for construction and large-scale application of existing or near-term CSP technology. The market share of CSP within the RE sector remains relatively small compared to PV, partly due to cost competitiveness and efficiency differences. While CSP offers advantages in energy storage through thermal storage systems, its efficiency levels, are lower than high-efficiency PV technologies, impacting its scalability in some regions [12]. In India, onshore wind energy dominates due to lower costs and existing infrastructure, while offshore wind is in the early development stage. Onshore turbines primarily use DD-EESG, GB-DFIG and GB-PMSG, offering moderate efficiency and capacity. Offshore turbines, including DD-PMSG, GB-PMG and GB-SCIG, are more efficient and larger in scale. Critical minerals like copper and high-strength alloys are essential, with offshore turbines requiring more REEs for permanent magnets. With India’s offshore wind expansion, demand for REEs is expected to rise, increasing import dependence, while copper's demands will also surge. Future advancements in superconducting generators and EESG could reduce REE dependence [13]. In the stationary battery energy storage sector, lithium-ion batteries dominate the market due to their high energy density, efficiency, and declining costs, with key chemistries including LFP. LFP batteries, known for their safety, thermal stability, and long cycle life, require more copper but eliminate the need for nickel and cobalt, making them geopolitically and environmentally favorable. They currently lead in utility-scale storage due to lower costs and reliability. NMC batteries, which have higher energy density than LFP but contain significant amounts of nickel, cobalt, and manganese, are preferred for residential and behind-the-meter storage applications. As the market shifts away from cobalt-rich chemistries, variants such as NMC 532, 622, and 811 being phased out completely. Vanadium flow batteries (VFBs) are emerging as a long-duration storage alternative, requiring large amounts of vanadium but offering nearly unlimited cycle life and high efficiency in large-scale renewable integration. Sodium-ion batteries, still in early commercialization, offer a lower-cost alternative with reduced mineral constraints, though they currently have lower energy density than lithium-ion counterparts. Future advancements, including solid-state batterie, are expected to enhance efficiency and reduce mineral dependency, though commercial viability remains a challenge. In electrolysers, although CETs have yet to reach full-scale market adoption, our projections indicate that post-2030, demand for Nickel in these technologies will surge, followed closely by Copper.

6. Conclusion

India's clean energy transition relies heavily on the availability of CMs essential for manufacturing renewable energy technologies. This study projects the demand for 31 CMs across five key renewable energy segments - Solar PV, CSP, Wind, BESS, and Green Hydrogen Electrolysers - until 2070. The findings indicate a substantial rise in YoY as well as cumulative mineral requirements, with Copper, Silicon, Graphite, Nickel, Phosphorous, Vanadium, Lithium, and Rare Earth Elements (REEs) emerging as the most critical due to their widespread application across multiple technologies. Given India's limited domestic reserves of several of these minerals, ensuring a stable and resilient supply chain is crucial for achieving its renewable energy goals. This study emphasizes the vast scale of critical mineral requirements for India's clean energy transition, highlighting the urgent need for resource efficiency strategies, domestic exploration, recycling initiatives, and strengthened international collaborations. Given that this study has ascertained the demand of critical minerals till 2070, future research would focus on the use of longitudinal data to optimize the supply of these critical minerals for India’s smooth transition to clean energy, thus reducing its vulnerability risk. The methodology would involve data-driven approach to optimize India’s import portfolio for critical minerals. A mixed (fixed and random) effects model could be employed to identify key determinants influencing India’s import patterns, variables such as production quantity, GDP (PPP, constant), electricity generation from renewables (excluding hydro, % of total), and governance index. Using the model’s coefficients, an import score would be generated for each source country, enabling the ranking of countries based on their suitability as import partners. This would be compared with a second import score derived from India’s actual import data. The comparison of these two rankings will yield an optimized import portfolio, distinguishing between countries India has historically imported from and those it should have prioritized based on performance and potential. This integrated approach would provide a foundation for strategic decision-making on critical mineral sourcing and trade partnerships, aligning India’s resource security with its long-term clean energy objectives. Together, the demand and supply analyses would offer a comprehensive perspective to guide India's policy formulation, investment planning, and international collaboration efforts, ensuring a resilient, sustainable, and self-reliant energy future.

Acknowledgement

A heartfelt gratitude towards NITI Aayog, Government of India for sharing important data, feedback and suggestions.

References

[1] Press Information Bureau, "Government declares plan to add 50 GW of renewable energy capacity annually for next 5 years to achieve the target of 500 GW by 2030," April 5, 2023. [Online]. Available: https://pib.gov.in/PressReleaseIframePage.aspx?PRID=1913789

[2] Press Information Bureau, "Net zero emissions target," August 3, 2023. [Online]. Available: https://pib.gov.in/PressReleaseIframePage.aspx?PRID=1945472

[3] International Energy Agency, Mineral Requirements for Clean Energy Transitions, IEA Publications, 2024. iea.org

[4] Ministry of Mines, Government of India, Annual Report 2022-23, June 2023. [Online]. Available: https://mines.gov.in/admin/download/649d4212cceb01688027666.pdf

[5] Australian Renewable Energy Agency, Technology Readiness Levels for Renewable Energy Sectors, Feb. 2014. [Online]. Available: https://arena.gov.au/assets/2014/02/Technology-Readiness-Levels.pdf

[6] M. H. A. Khan, T. Sitaraman, N. Haque, G. Leslie, S. Saydam, R. Daiyan, et al., "Strategies for life cycle impact reduction of green hydrogen production – Influence of electrolyser value chain design," International Journal of Hydrogen Energy, vol. 62, pp. 769–782, 2024.

[7] E. Schropp, G. Naumann, and M. Gaderer, "Hydrogen production via solid oxide electrolysis: Balancing environmental issues and material criticality," Advances in Applied Energy, vol. 16, p. 100194, 2024.

[8] R. Whitlock, "Rethink Energy publishes solar perovskite forecast to 2040," Renewable Energy Magazine, Sep. 18, 2024.

[9] C. Konda and K. Rakheja, "India's hunt for critical minerals," Institute for Energy Economics and Financial Analysis, Oct. 28, 2024. [Online]. Available: https://ieefa.org/sites/default/files/2024-10/India%27s%20Hunt%20for%20Critical%20Minerals.pdf

[10] S. Passerini, L. Barelli, M. Baumann, J. Peters, and M. Weil, Emerging Battery Technologies to Boost the Clean Energy Transition: Cost, Sustainability, and Performance Analysis. Cham: Springer Nature, 2024, p. 337.

[11] K. Ranabhat, L. Patrikeev, A. A. E. Revina, K. Andrianov, V. Lapshinsky, and E. Sofronova, “An introduction to solar cell technology,” Journal of Applied Engineering Science, vol. 14, no. 4, 2016.

[12] E. Pihl, D. Kushnir, B. Sandén, and F. Johnsson, “Material constraints for concentrating solar thermal power,” Energy, vol. 44, no. 1, pp. 944–954, 2012.

[13] R. Chadha and G. Sivamani, “Projecting critical minerals need for India’s energy transition: How much of which minerals are needed for the transition?,” Working Paper: Minerals & Mining, Centre for Social and Economic Progress, Jun. 7, 2024.

[14] L. Wagner, J. Suo, B. Yang, D. Bogachuk, E. Gervais, R. Pietzcker, et al., “The resource demands of multi-terawatt-scale perovskite tandem photovoltaics,” Joule, vol. 8, no. 4, pp. 1142–1160, 2024.

[15] V. S. Prabhu, S. Shrivastava, and K. Mukhopadhyay, “Life cycle assessment of solar photovoltaic in India: A circular economy approach,” Circular Economy and Sustainability, pp. 1–28, 2022.

[16] E. Pihl, D. Kushnir, B. Sandén, and F. Johnsson, “Material constraints for concentrating solar thermal power,” Energy, vol. 44, no. 1, pp. 944–954, 2012.

[17] S. Carrara, P. Alves Dias, B. Plazzotta, and C. Pavel, Raw Materials Demand for Wind and Solar PV Technologies in the Transition Towards a Decarbonised Energy System. Luxembourg: Publications Office of the European Union, 2020.

[18] L. McGovern, E. Tapoglou, and A. Georgakaki, “Material requirements for wind turbines,” JRC Report No. JRC139701, European Commission, Nov. 27, 2024. [Online]. Available: https://publications.jrc.ec.europa.eu/repository/bitstream/JRC139701/JRC139701_01.pdf

[19] International Energy Agency, Energy Technology Perspectives 2023, Paris: IEA, Jan. 2023. [Online]. Available: https://iea.blob.core.windows.net/assets/a86b480e-2b03-4e25-bae1-da1395e0b620/EnergyTechnologyPerspectives2023.pdf

[20] Y. Xiao, J. Xiao, H. Zhao, J. Li, G. Zhang, D. Zhang, et al., “Prussian blue analogues for sodium-ion battery cathodes: A review of mechanistic insights, current challenges, and future pathways,” Small, vol. 20, no. 35, p. 2401957, 2024.

[21] H. Liao, Z. Zhang, Y. Zheng, and Y. Gao, “$NaFePO_4$ for sodium-ion batteries: Mechanism, synthesis and optimization strategies toward commercialization,” Energy Storage Materials, vol. 65, p. 103157, 2024.

[22] B. Pandit, M. Johansen, C. S. Martínez-Cisneros, J. M. Naranjo-Balseca, B. Levenfeld, D. B. Ravnsbæk, and A. Varez, “$Na_3V_2(PO_4)_3$ cathode for room-temperature solid-state sodium-ion batteries: Advanced in situ synchrotron X-ray studies to understand intermediate phase evolution,” Chemistry of Materials, vol. 36, no. 5, pp. 2314–2324, 2024.

[23] J. Jiang, G. Huang, and W. Yao, "High stability $Na_{0.7}MnO_{2.05}$ cathode for sodium-ion batteries," Materials Chemistry and Physics, vol. 296, p. 127307, 2023.

[24] C. M. Julien and A. Mauger, "Fabrication of $Li_4Ti_5O_{12}$ (LTO) as anode material for Li-ion batteries," Micromachines, vol. 15, no. 3, p. 310, 2024.

[25] B. Teixeira, M. C. Brito, and A. Mateus, "Strategic raw material requirements for large-scale hydrogen production in Portugal and European Union," Energy Reports, vol. 12, pp. 5133–5144, 2024.

[26] International Energy Agency, "Estimated levelised demand for selected minerals in electrolysers and fuel cells today (log scale)," May 5, 2021. [Online]. Available: https://www.iea.org/data-and-statistics/charts/estimated-levelised-demand-for-selected-minerals-in-electrolysers-and-fuel-cells-today-log-scale.

[27] J. C. Koj, C. Wulf, A. Schreiber, and P. Zapp, "Site-dependent environmental impacts of industrial hydrogen production by alkaline water electrolysis," Energies, vol. 10, no. 7, p. 860, 2017.

[28] Grand View Research, Inc., India Solar PV Panels Market Size, Share & Trends Analysis Report by Technology (Thin Film, Crystalline Silicon), by Grid (On-Grid, Off-Grid), by Application (Residential, Commercial, Industrial), and Segment Forecasts, 2024–2030, Report ID: GVR-4-68040-307-2, Grand View Research, 2024. [Online]. Available: https://www.grandviewresearch.com/industry-analysis/india-solar-pv-panels-market-report

[29] C. Del Pero, N. Aste, F. Leonforte, and F. Sfolcini, "Long-term reliability of photovoltaic c-Si modules – A detailed assessment based on the first Italian BIPV project," Solar Energy, vol. 264, p. 112074, 2023.

[30] S. De Wolf, A. Descoeudres, Z. C. Holman, and C. Ballif, "High-efficiency silicon heterojunction solar cells: A review," Green, vol. 2, no. 1, pp. 7–24, 2012.

[31] Fortune Business Insights, Concentrated Solar Power (CSP) Market Size, Share & Industry Analysis by Technology (Parabolic Trough, Power Tower, Linear Fresnel), by Application (Residential, Non-Residential, Utility) and Regional Forecasts, 2024–2032, Report ID: FBI100751, Sep. 1, 2025.

[32] Grand View Research, Inc., Concentrated Solar Power (CSP) Market Size, Share & Trends Analysis Report by Technology (Parabolic Trough, Linear Fresnel, Dish, Power Tower), by Application, by Region, and Segment Forecasts, 2025–2030, Grand View Research, 2024. [Online]. Available: https://www.grandviewresearch.com/industry-analysis/concentrated-solar-power-csp-market

Appendix

1. Material Intensity

1.1. Mineral Intensities (in t/GW) of Solar PV Technologies [13,14,15]

Technologies	Catagories	TRL	Nickel (Ni)	Tin (Sn)	Copper (Cu)	Silicon (Si)	Indium (In)	Gallium (Ga)	Selenium (Se)	Cadmium (Cd)	Tellurium (Te)	Molybdenum (Mo)	Tungsten (W)	Graphite	Titanium (Ti)	Lithium (Li)	Germanium (Ge)
Monocrystalline Silicon (mono-Si) PV	c-Si	9			4600	4000											
Polycrystalline Silicon (poly-Si) PV		9			4600	4000											
Heterojunction Silicon (HJT) PV		9			4600	4000											
Copper Indium Gallium Selenide (CIGS) Thin-Film PV	Thin film	9		6	4622		15	4	35	0		0					
Amorphous Silicon (a-Si) Thin-Film PV		9			4600	150											48
Cadmium Telluride (CdTe)		9		103.3	4600					50	52	0					
perovskite/silicon tandem	Perovskite	5	0.132	0.456	0		2.259					0	0	0	0.972	0	
Perovskite APT		4	3.223	12.509	2.987		4.707					3.427	6.417	143.733	1.944	0.0024	

1.2. Mineral Intensities (in t/GW) of Solar CSP Technologies [16]

Solar CSP Technology	**Categories**	**Copper (Cu)**	**Molybdenum (Mo)**	**Nickel (Ni)**	**Titanium (Ti)**	**Vanadium (V)**	**Niobium (Nb)**
Parabolic troughs	**Linear concentrating systems**	3200	200	940	25	1.9	650
Solar power towers	**Point Focus**	1400	56	1800	0	1.7	1400

1.3. Mineral Intensities (in t/GW) of Onshore & Onshore Wind Technologies [17-18]

Technologies	Classification	Broad Category	Wind turbine types	Copper (Cu)	Dysprosium (Dy)	Molybdenum (Mo)	Neodymium (Nd)	Nickel (Ni)	Praseodymium (Pr)	Terbium (Tb)	yttrium (Y)
GB-HS-PMSG (GB HS PMG)	Onshore	Gearbox	Gearbox High Speed Permanent Magnet Synchronous Generator	1150	7	110	70	490	4	1	
GB-DFIG		Gearbox	Gearbox Doubly-Fed Induction Generator	1900	3	110	18	490	0	0	
GB-SCIG		Gearbox	Gearbox-Squirrel Cage Induction Generator	1000	4.7	110	34	490	0	0	
DD-EESG		Direct Drive	Direct Drive Electrically Excited Synchronous Generator	6200	0	110	0	490	0	0	
DD-PMSG		Direct Drive	Direct Drive Permanent Magnet Synchronous Generator	4600	21	110	210	490	35	7	
GB-SCIG	Offshore	Gearbox	Gearbox-Squirrel Cage Induction Generator	1000	4.7	110	34	490	0	0	
DD-PMSG		Direct Drive	Direct Drive Permanent Magnet Synchronous Generator	4600	21	110	210	490	35	7	
DD-HTS		Direct Drive	Direct Drive High tempreture semiconductore	6200	0	110	0	490	0	0	0.3
GB-MS PMG		Gearbox	Gearbox Medium Speed Permanent Magnet Synchronous Generator	1150	7	110	70	490	4	1	

1.4. Mineral Intensities (in t/GWh) of BESS Technologies [10,13, 19-24]

Technologies	Battery types	Graphite	Lithium (Li)	Cobalt (Co)	Nickel (Ni)	Copper (Cu)	Vanadium	Titanium (Ti)	Phosphorous (P)
Prussian Blue Analogues ($Na_2Fe[Fe(CN)_6]$)	(PBA)				580				
NASICON ($Na_3V_2(PO_4)_3$)	NVP						598		545
Vanadium Redox Flow Battery	VRFB					21	3400		
Lithium Nickel Manganese Cobalt	NMC 523	883	117	183	467				
Lithium Titanate	LTO		54					469	
Lithium Iron Phosphate	LFP	1100	87	0	0	433			387
Sodium Iron Phosphate ($NaFePO_4$)	NFP								457
Lithium Nickel Manganese Cobalt	LNMC-811	750	83	83	650	333			
Layered Sodium Manganese Oxide ($NaMnO_2$)	NaMO2								
Sodium Nickel Manganese Cobalt	NaNMC			83	650				

Lithium Nickel Manganese Cobalt	LNMC-622	883	100	183	533	317
Sodium-Nickel Chloride	NaNiCl2				1500	
Polysulfide Bromide	PSB					
Solid-State Batteries	ESS		200			
Sodium-Sulfur	NaS					
Lithium-Sulfur Batteries	Li–S		200			
Zinc-Bromine	ZnBr					

1.5. Mineral Intensities (in t/GW) of Electrolysers for Green Hydrogen [6,7,25-27]

Technology	TRL	Copper (Cu)	Zirconium (Zr)	Nickel (Ni)	Graphite	Cobalt (Co)	Iridium (Ir)	Platinum (Pt)	Silicon (Si)	Titanium (Ti)	Lanthanum (La)	Strontium (Sr)	Gadolinium(Gd)	Cerium (Ce)	Yttrium (Y)
alkaline electrolysers (AEL)	Mature [8-9]	533.33	245	5066.67	114.67	8									
proton exchange membrane electrolysers (PEMEL)	Commercial [8-9]	0.53			1.7		1.4	0.19	1.05	0.61					
solid oxide electrolysis (SOEL)	Demonstration [5-6]	14.149	0.90761	1.791					14.149	6.5084	1.2882	0.038128	0.0053167	0.01895	0.062563

2. Year-on-Year Capacity

2.1. New Capacity of Solar PV, CSP, Wind, BESS, & Electrolysers under BAU

Year	2030	2035	2040	2045	2050	2055	2060	2065	2070
Solar PV (GW)	195.81-239.32	212.02-259.14	225.61-275.75	318.02-388.69	447.78-547.29	554.67-677.93	554.32-677.50	739.33-903.63	739.14-903.39
Solar CSP (GW)	0.39-0.47	0.37-0.46	0.28-0.34	0.57-0.70	1.31-1.60	1.53-1.86	1.87-2.29	3.16-3.86	3.36-4.11
Onshore Wind (GW)	52.2-63.8	79.2-96.8	108-132	144.9-177.1	167.4-204.6	192.6-235.4	192.6-235.4	222.3-271.7	264.6-323.4
Offshore Wind (GW)	0.9-1.1	3.6-4.4	3.6-4.4	8.1-9.9	8.1-9.9	11.7-14.3	11.7-14.3	12.6-15.4	11.7-14.3
BESS (GWh)	25.2-30.8	54-66	51.3-62.7	189-231	247.5-302.5	327.6-400.4	369-451	421.2-514.8	348.3-425.7
Green Hydrogen Electrolysers (Mt)	1.8-2.2	0.9-1.1	1.8-2.2	1.8-2.2	3.6-4.4	3.6-4.4	4.5-5.5	5.4-6.6	8.1-9.9

2.2. New Capacity of Solar PV, CSP, Wind, BESS, & Electrolysers under NZ

Year	2030	2035	2040	2045	2050	2055	2060	2065	2070
Solar PV (GW)	214.86-262.61	365.03-446.15	376.85-460.59	571.80-698.87	665.67-813.60	936.22-1144.27	935.77-1143.73	1389.21-1697.92	1388.92-1697.56
Solar CSP (GW)	0.23-0.29	0.36-0.44	0.25-0.30	0.59-0.72	1.22-1.49	1.57-1.92	2.02-2.47	3.98-4.87	4.28-5.23
Onshore Wind (GW)	82.8-101.2	108.9-133.1	136.8-167.2	187.2-228.8	221.4-270.6	218.7-267.3	261-319	309.6-378.4	398.7-487.3
Offshore Wind (GW)	0.9-1.1	3.6-4.4	3.6-4.4	8.1-9.9	8.1-9.9	11.7-14.3	12.6-15.4	17.1-20.9	18-22
BESS (GWh)	118.8-145.2	82.8-101.2	170.1-207.9	440.1-537.9	539.1-658.9	520.2-635.8	738.9-903.1	851.4-1040.6	1383.3-1690.7
Green Hydrogen Electrolysers (Mt)	3.6-4.4	2.7-3.3	3.6-4.4	6.3-7.7	10.8-13.2	8.1-9.9	9-11	11.7-14.3	16.2-19.8

2.3. Proportion of Solar PV and Solar CSP

Year	2030	2035	2040	2045	2050	2055	2060	2065	2070
					BAU				

Solar PV	0.998	0.998	0.999	0.998	0.997	0.997	0.997	0.996	0.995
CSP	0.0020	0.0018	0.0013	0.0018	0.0029	0.0028	0.0034	0.0043	0.0045
					NZ				
Solar PV	0.999	0.999	0.999	0.999	0.998	0.998	0.998	0.997	0.997
CSP	0.0011	0.0010	0.0007	0.0010	0.0018	0.0017	0.0022	0.0029	0.0031

3. Market Share of each low-carbon technology (2030-2070)

Year	**2025**	**2030**	**2035**	**2040**	**2045**	**2050**	**2055**	**2060**	**2065**	**2070**
					Solar PV Technology (under BAU) [11,14,28-30]					
Monocrystalline Silicon (mono-Si) PV	54%	52%	49%	45%	42%	40%	38%	36%	34%	32%
Polycrystalline Silicon (poly-Si) PV	30%	27%	25%	22%	20%	19%	18%	17%	17%	17%
Heterojunction Silicon (HJT) PV	8%	10%	12%	14%	15%	17%	18%	19%	19%	19%
Copper Indium Gallium Selenide (CIGS) Thin-Film PV	2%	3%	4%	5%	6%	7%	8%	9%	11%	12%
Amorphous Silicon (a-Si) Thin-Film PV	3%	2%	2%	1%	1%	1%	1%	1%	0%	0%
Cadmium Telluride (CdTe)	3%	5%	6%	7%	7%	7%	7%	8%	8%	8%
Perovskite/silicon tandem	0%	0%	2%	4%	5%	6%	6%	7%	7%	8%
Perovskite APT	0%	0%	0%	3%	4%	5%	5%	5%	5%	5%
					Solar PV Technology (under NZ) [11,14,28-30]					
Monocrystalline Silicon (mono-Si) PV	54%	50%	45%	40%	35%	32%	28%	26%	25%	24%
Polycrystalline Silicon (poly-Si) PV	30%	28%	24%	19%	15%	12%	10%	8%	7%	5%
Heterojunction Silicon (HJT) PV	8%	10%	13%	15%	17%	18%	19%	20%	20%	20%
Copper Indium Gallium Selenide (CIGS) Thin-Film PV	2%	5%	6%	7%	9%	11%	13%	14%	15%	16%
Amorphous Silicon (a-Si) Thin-Film PV	3%	1%	1%	1%	1%	1%	1%	0%	0%	0%
Cadmium Telluride (CdTe)	3%	6%	7%	9%	11%	12%	13%	13%	13%	13%
Perovskite/silicon tandem	0%	0%	4%	5%	7%	8%	9%	10%	11%	11%
Perovskite APT	0%	0%	0%	4%	5%	6%	7%	8%	10%	11%
					Solar CSP (Under BAU) [31-32]					
Parabolic troughs	95%	94.00%	91.00%	89.00%	87.00%	86.00%	84.00%	82.00%	81.00%	80.00%
Solar power towers	5%	6.00%	9.00%	11.00%	13.00%	14.00%	16.00%	18.00%	19.00%	20.00%
					Solar CSP (Under NZ) [31-32]					
Parabolic troughs	85%	75.00%	55.00%	45%	35.00%	30.00%	25%	22.00%	21.00%	20.00%
Solar power towers	15%	25.00%	45.00%	55%	65.00%	70.00%	75%	78.00%	79.00%	80.00%
					Onshore Wind (Under BAU) [17]					
GB-HS-PMSG (GB HS PMG)	35%	37%	39%	40%	41%	42%	42%	42%	43%	43%
GB-DFIG	25%	22%	19%	15%	13%	11%	10%	9%	7%	6%
GB-SCIG	2%	1%	1%	1%	1%	1%	1%	1%	1%	1%
DD-EESG	30%	32%	33%	34%	35%	35%	36%	37%	38%	39%
DD-PMSG	7%	8%	9%	10%	11%	11%	11%	12%	12%	12%
					Onshore Wind (Under NZ) [17][Error! Bookmark not defined.]					
GB-HS-PMSG (GB HS PMG)	42%	43%	44%	45%	45%	45%	45%	45%	45%	45%
GB-DFIG	8%	7%	4%	3%	1%	0%	0%	0%	0%	0%
GB-SCIG	2%	1%	1%	0%	0%	0%	0%	0%	0%	0%
DD-EESG	24%	24%	25%	26%	27%	27%	27%	27%	27%	27%
DD-PMSG	24%	25%	26%	26%	27%	27%	27%	28%	28%	28%
					Offshore Wind (Under BAU) [17]					
GB-SCIG	57%	57%	56%	54%	52%	50%	48%	45%	45%	45%
DD-PMSG	31%	31%	30%	29%	27%	26%	25%	25%	25%	24%
DD-HTS	0%	0%	2%	5%	8%	11%	14%	17%	17%	17%

GB-MS PMG	12%	12%	12%	12%	13%	13%	13%	13%	13%	14%
Offshore Wind (Under NZ) [17]										
GB-SCIG	6%	5%	5%	5%	4%	4%	3%	3%	3%	3%
DD-PMSG	75%	82%	84%	85%	86%	87%	88%	88%	88%	88%
DD-HTS	0%	0%	0%	0%	0%	0%	0%	0%	0%	0%
GB-MS PMG	18%	12%	11%	11%	10%	10%	9%	9%	9%	9%
BESS (same market share under BAU and NZ) [10,19]										
Lithium Iron Phosphate	90%	86.0%	80.0%	75.2%	70.3%	65.8%	61.2%	56.5%	51.4%	46.1%
NMC 523	2%	0.2%	0.0%	0.0%	0.0%	0.0%	0.0%	0.0%	0.0%	0.0%
NMC 811	2%	1.5%	0.0%	0.0%	0.0%	0.0%	0.0%	0.0%	0.0%	0.0%
NMC 622	2%	1.1%	0.0%	0.0%	0.0%	0.0%	0.0%	0.0%	0.0%	0.0%
Lithium Titanate	0%	0.9%	1.5%	2.1%	2.7%	3.3%	3.9%	4.5%	5.1%	5.7%
Sodium Iron Phosphate ($NaFePO_4$)	0%	1.0%	2.0%	2.3%	2.6%	3.0%	3.3%	3.7%	4.1%	4.4%
Prussian Blue Analogues ($Na_2Fe[Fe(CN)_6]$)	0%	1.0%	2.0%	2.3%	2.6%	3.0%	3.3%	3.7%	4.1%	4.4%
NASICON ($Na_3V_2(PO_4)_3$	0%	1.0%	2.0%	2.3%	2.6%	3.0%	3.3%	3.7%	4.1%	4.4%
Layered Sodium Manganese Oxide ($NaMnO_2$)	0%	1.0%	2.0%	2.3%	2.6%	3.0%	3.3%	3.7%	4.1%	4.4%
Sodium Nickel Manganese Cobalt	0%	1.0%	2.0%	2.3%	2.6%	3.0%	3.3%	3.7%	4.1%	4.4%
Sodium-Nickel Chloride	1%	1.0%	1.5%	2.0%	2.4%	2.6%	2.8%	3.0%	3.2%	3.4%
Sodium-Sulfur	1%	1.0%	1.4%	1.8%	2.2%	2.4%	2.6%	2.8%	3.0%	3.2%
Vanadium Redox Flow Battery	1%	1.5%	1.8%	2.1%	2.4%	2.7%	3.0%	3.3%	3.6%	4.0%
Polysulfide Bromide	1%	0.8%	1.2%	1.6%	2.0%	2.4%	2.8%	3.2%	3.6%	4.0%
Zinc-Bromine	1%	0.8%	1.2%	1.6%	2.0%	2.4%	2.8%	3.2%	3.6%	4.0%
Solid-State Batteries	0%	0.2%	0.4%	0.6%	1.0%	1.4%	1.8%	2.2%	2.6%	4.0%
Lithium-Sulfur Batteries	0%	0.0%	1.0%	1.4%	1.8%	2.2%	2.6%	3.0%	3.4%	3.8%
Electrolysers (same market share under BAU and NZ) [10,19]										
alkaline electrolysers (AEL)	65%	65%	60%	55%	50%	45%	40%	35%	30%	25%
proton exchange membrane electrolysers (PEMEL)	23%	25%	27%	28%	29%	30%	31%	32%	33%	34%
solid oxide electrolysis (SOEL)	10%	10%	13%	17%	21%	25%	29%	33%	37%	41%